DEVELOPMENT AND EVALUATION OF 3D BIO-PRINTED CANCER TISSUE CONSTRUCT FOR DRUG TESTING

THESIS SUBMITTED BY

Ms. RENCY GEEVARGHESE

IN PARTIAL FULFILLMENT OF THE REQUIREMENTS FOR THE DEGREE OF MASTER OF PHILOSOPHY

SREE CHITRA TIRUNAL INSTITUTE FOR MEDICAL SCIENCES AND TECHNOLOGY
THIRUVANANTHAPURAM – 695011

DECLARATION

I, **Ms. Rency Geevarghese**, hereby declare that the thesis work entitled '**Development and Evaluation of 3D Bio-printed Cancer Tissue Construct for Drug Testing**' was done by me under the direct guidance of **Dr. Renjith P. Nair, Scientist C, Division of Thrombosis Research**, Biomedical technology wing, Sree Chitra Tirunal Institute for Medical Sciences and Technology, Thiruvananthapuram, Kerala, India. External help sought are acknowledged.

Ms. RENCY GEEVARGHESE

2019/MPhil/02

SREE CHITRA TIRUNAL INSTITUTE FOR MEDICAL SCIENCES AND TECHNOLOGY
THIRUVANANTHAPURAM – 695011, INDIA
(An institute of national importance under Govt. of India)

CERTIFICATE

This is to certify that the thesis work entitled '**Development and Evaluation of 3D Bio-printed Cancer Tissue Construct for Drug Testing**' submitted by Ms.Rency Geevarghese (2019/M.Phil/02) in partial fulfillment for the Degree of Mater of Philosophy in Biomedical Technology was done under my supervision and guidance at **Division of Thrombosis Research**, Biomedical technology wing, Sree Chitra Tirunal Institute for Medical Sciences and Technology, Thiruvananthapuram, Kerala, India.

Place: Thiruvananthapuram
Date: 28/07/2020

Dr. Renjith P. Nair

Dr. RENJITH P. NAIR, Ph.D
Scientist C
Division of Thrombosis Research
Department of Applied Biology
Bio Medical Technology Wing
SCTIMST, Thiruvananthapuram-12

The Thesis Entitled

DEVELOPMENT AND EVALUATION OF 3D BIO- PRINTED CANCER TISSUE CONSTRUCT FOR DRUG TESTING

Submitted by

Ms. Rency Geevarghese

In partial fulfillment of the requirements for the degree of

MASTER OF PHILOSOPHY

Of

SREE CHITRA TIRUNAL INSTITUTE FOR MEDICAL SCIENCES AND TECHNOLOGY, THIRUVANANTHAPURAM – 695011, INDIA

Evaluated and approved by

28/07/2020

Dr. Renjith P. Nair

(Supervisor)

Dr. RENJITH P. NAIR, Ph.D
Scientist C
Division of Thrombosis Research
Department of Applied Biology
Bio Medical Technology Wing
SCTIMST, Thiruvananthapuram-12

28.07.2020.

Signature

Examiner's name and designation

Dr. Anil Kumar PR
Scientist F

ACKNOWLEDGEMENT

First of all I would like to thank God Almighty, for showering his blessings to complete my work successfully.

This study was carried out under the supervision and valuable guidance of my guide Dr. Renjith P. Nair, Scientist C, Division of Thrombosis Research, Biomedical Technology Wing, SCTIMST, Trivandrum. I gratefully acknowledge the excellent and incessant help given by him, and, for his valuable guidance and encouragement throughout this study and for the correction of the thesis.

I am grateful to Dr. Anugya Bhatt, Scientist in Charge (TRU), BMT Wing, for her generosity and sincere help rendered throughout the tenure of the MPhil Course.

I would like to express my gratitude to The Director SCTIMST, Head BMT Wing, Registrar and M.Phil Coordinator for their co-operation, encouragement and providing all the support during the work.

I would also like to extend my sincere thanks to Dr Naresh Kasoju (TIC) and Dr. Rekha. M.R (BST) for their guidance and reagents endorsed for the study.

I would like to give special thanks to Dr. Anugya Bhatt, Ms. Lakshmi T S, Ms Riya Rayu and Mr Suvanish S Kumar for their support and guidance for bio ink formulation and help in 3D bio printing. I would also like to thank Ms. Deepa S for all her help in cell culture, Dr. Anil Kumar and Team (Cytotoxicity Testing), Mr Nishad (SEM analysis) and Mr. Deepu (MicroCT analysis).

I am also grateful to the whole hearted support rendered by members Division of Thrombosis Research Mr. Renjith S Kartha, Mr. Anil, Ms. Priyanka, Ms. Renu, Ms. Shafina, MS. Deepa S, Ms. Subha, Ms. Athira, and Ms. Reshmi.

I would like to thank my Parents, Husband and Friends for their encouragement and co-operation.

- RENCY GEEVARGHESE

TABLE OF CONTENTS:

LIST OF FIGURES:

Synopsis:

Literature suggests that 90% of anticancer drugs that pass through preclinical drug screening end up failing during clinical trials. This is mainly due to lack of effective drug screening systems. Studies showed that 3D bio-printed construct can serve as a better drug screening model with added on advantage over the traditional 2D screening system. 3D drug screening model with excellent biomimetic properties that overcome the limitations of the conventional 2D culture system is the need of the hour.

The current study focused on the development of a novel bio ink (AGDCelCp) formulation constituting Sodium Alginate cross-linked with Calcium ions, Gelatin, Diethyl Amino ethyl (DEAE) Cellulose, and Collagen Peptide for the development of 3D cancer tissue construct for drug screening applications. In this study, we exemplify the fabrication of a 3D printed lung cancer tissue model by encapsulating A549 human cell line (non-small cell lung cancer cell line) in the developed bio ink.

The study primarily involves the optimization of the bio ink formulation, printability optimization of bio-ink, and fabrication of 3D bio-printed construct. Further, the physical, chemical, and morphological characterization of the printed construct was studied followed its cyto-compatibility evaluation. The qualitative and quantitative assay was performed to assess the ability of the 3D bio-printed construct to support cellular growth and proliferation. Proof of concept study was also carried out to evaluate the suitability of this 3D bio-printed construct as a drug screening model.

The study is presented in five Chapters.

Chapter I includes an introduction to the research topic, review of the work done so far related to the proposed study. Introducing emphasis on the significance of the study in the current situation, the need for such a bio ink model and its implication. Following introducing, the review part gives an overview of drug screening models ranging from in vivo system to in vitro models and elucidating the recent trends in drug toxicity testing. Then, an outline of anticancer drug screening and currently used 3D models in cancer studies are detailed. The chapter then elucidate 3D bio printing technology and bio-ink, the implication of 3D bio printing in cancer study, lung cancer study, and the use of 3D bio-printed construct in drug screening. It also explains various components used in this bio ink system and its advantages over the trending bio ink system. Further, based on this, the gap area was identified and clear objectives were formed.

Chapter II gives details of the materials and methods used in each study. The chapter mainly explains the procedure involved in the optimization of bio ink formulation, development of 3D bio-printed tissue construct, characterization, cytotoxicity assay, evaluation of 3D bio-printed construct, and preliminary drug testing of the 3D bio-printed construct.

Chapter III illustrates the results using figures, tables and graphs. In this chapter the suitability of developed bio ink for 3D bio printing of cancer tissue construct is demonstrated. The suitability of bio-printed construct as a drug screening model was also demonstrated. In Chapter IV results are discussed in light of literature and importance of current study is highlighted. Chapter V

summarises the results and consists of a conclusion which gives an idea about the shortcoming of the study and its future prospective followed by bibliography.

Chapter I

1.1 Introduction:

The advent of 3D bio-printing has opened up a whole new avenue in the field of tissue engineering and cytological evaluation. With the introduction of this additive manufacturing technology, a drastic shift has been observed from the conventional 2D culture to 3D construct with a promising feature to mimic the physiological environment. The taking over of 3D bio-printing technology has encouraged the scientific community to explore numerous bio-ink formulation and fabricate various tissue constructs that best serve the purpose. Though several bio-ink formulations with excellent printability, biocompatibility and degradation have been studied for the past two decades, however, the challenge persists to develop an ideal bio-ink system.

Studies have proved that around 90% of the anticancer drug that passes through pre-clinical drug screening ends up as a failure. One of the main reason for the drug attrition is due to the inability of the study model to bio-mimic the physiological microenvironment. Thus, the current situation demands the need for a 3D bio-printed drug testing model. This model owes an obvious extended implications in cancer therapy.

The study proposes the fabrication of a novel bio-ink (AGDCelCp) that constitute of Calcium cross-linked Sodium Alginate, Gelatin, DEAE (Diethyl Aminoethyl) Cellulose and Collagen Peptide. Briefly, the advantage of this hybrid bio-ink system is primarily due to the electrostatic interaction between Sodium Alginate-Gelatin, DEAE Cellulose-Sodium Alginate, and DEAE Cellulose-Cell

surface. The presence of Collagen peptide upgrades the cell proliferation and adhesion property of the system and also provide biomimetic cues. Also, the structural stability and longevity of the bio-ink is elevated due to the presence of DEAE Cellulose and Calcium ions in the dispersion medium. Since all of these components releases non-cytotoxic product on degradation it shows excellent biomimetic and biocompatible property.

The study commences with optimization of concentration of bio-ink (AGDCelCp) component and bio printing parameters for fabrication of a 3D bio-printed tissue construct with A549 cells. The physical, chemical and morphological characterization of the 3D printed construct was studied following its cyto-compatibility testing. The 3D printed construct with A549 cells was then cultured in DMEM F12 media to evaluate the constructs' ability to endorse cell growth and proliferation. The evaluation of the 3D bio-printed construct was performed both qualitatively (by Live Dead Assay and H-E Staining) and quantitatively (via MTT Assay). The last phase of the study involves the preliminary validation of the 3D bio-printed construct as a drug screening model.

In a nutshell, the study recapitulates the development and evaluation of a 3D printed cancer tissue construct to prove its efficacy as a drug testing model.

1.2 Review of Literature:

1.2.1 Drug Toxicity Testing:

Drug toxicity testing holds a pivotal role in pharmaceutical and therapeutic facet of research. Drug toxicity testing involves the screening of an identified product to prove its efficacy as a therapeutic tool. Conventionally, both

in vitro and *in vivo* toxicity testing are employed for this pre-selection process (Kumar, *et al* 2016). In the paper titled "Preclinical screening of new anticancer agents" Angelika M. Burger elucidates that screening aims to 'identify a compound with anti-tumor effects and define the product that matches the criteria thereby progressing it to the next stage of preclinical development'. The major components of the strategy include the chemical characterization of the drug, toxicity testing, dose response and extrapolating the models (Soldatow *et al.*, 2013). An ideal method for screening involves a combination of speed, simplicity and low costs with optimal predictability of pharmacodynamics activity (Lewis,*et al* 2012).

1.2.2 Recent Trends in Drug Toxicity Testing:

Though the drug screening methods adapted differ depending on its tissue specificity the basic idea behind these models is to reduce the attrition to drug failure and recreate the physiological condition. Zebra fish is considered as a desirable preclinical *in vivo* model for drug screening. The ease of maintenance and drug administration, short reproductive cycle and transparency allowing its visual assessment of developing cells and organs are some of the reasons why it is preferred over other animals (Parng *et al.*, 2002).

The main objective of early *in vivo* preclinical evaluation is to characterize the potential adverse effect and safety margin of the drug. Thus, answering the question if the compound is safe for human use or whether to eliminate it from further development. Retrospective industrial studies have indicated that the predictability of *in vivo* models to human toxicities is quite

misleading. While rodent and non-rodents show predictability of 43% and 63% respectively, the combination of these two species can predict approximately 71% to human toxicities (Olson *et al.*, 2000).The relevancy and accuracy of this strategy are yet suspected when it comes to a novel product.

Another crucial aspect that has to overlook is the huge sum of amount and time invested for drug launching in a market. It takes approximately 12 to 15 years costing around 3-5 billion for drug identification, optimization followed by human clinical trials and its final introduction into the market (DiMasi, *et al* 2003).A major cause for the steady rise in the cost of drug development is the late stage attrition of the approved drug (Frantz, *et al* 2003).Therefore, an efficiently engineered system with an improvised method of measurement, better understanding of its mechanism of toxicity and reliance on biomarkers can turn the *in vivo* studies invaluable by early prioritization and selection.

1.2.3 Models and methods adopted for *in vitro* toxicity study

While *in vivo* models were considered as the gold standard for assessing human risk, the advent of *in-silico* and *in vitro* models have brought about a drastic change in the scenario. The *in vitro* model consumes less time, effort and money than chemical toxicity testing performed on *in vivo* models. The system mimics physiological microenvironment via better cell-cell, cell- ECM, exposure to cell fate determinants and rapid performance of cytotoxicity assay (Zucco *et al.*, 2004). It also enhances the sensitivity and accuracy of identifying the end stage events. The diversity of the genotype of animals further complicates the replication of the

study (Jain *et al.*, 2018).

Some of the widely acceptable *in vitro* cytotoxicity models are 2D cell culture, 2D co-culture, 3D culture model, tissue slice or grafting model and micro scale or microfluidic cell culture model (Mahto, *et al* 2010). Each of these models has its advantage and disadvantages. Varied cell parameters can be used to evaluate the cytological damage and given below is a tabular representation of it (Table 1). Also other test like mutagenicity (Galloway, *et al* 1994), toxicokinetic study (Godoy *et al* , 2012) and cellular and functional response (protein/gene expression) (Li *et al.*, 2008) can be used for follow up studies. Moreover, some of the recent approaches used in *in vitro* evaluation is the integration of omics (Debnath *et al.*, 2010b), bioinformatics and computational tools (Debnath *et al.*, 2010a).

Table 1 : Common endpoints used in cytotoxicity analysis	
Cell parameter	**Cytotoxicity assay**
Cell number	Trypan Blue (Oliver *et al.*, 1989) Methylene Blue assay (Oliver *et al.*, 1989) ALP assay(Oliver *et al.*, 1989) Sulforhodamine assay (Mahto, Chandra and Rhee, 20 Resazurin (Oliver *et al.*, 1989)
Cell viability	LDH assay (Mahto, Chandra and Rhee, 2010) Alamar Blue assay (Oliver *et al.*, 1989) MTT assay (Mahto, Chandra and Rhee, 2010) Fluorescein Diacetate (Lecoeur *et al.*, 2001) Calcein AM (Lecoeur *et al.*, 2001) Annexin (Lecoeur *et al.*, 2001) Granzyme based assay (Bird *et al.*, 2005) Caspase based assay (Reddivari *et al.*, 2007)
Nuclear structure Nuclear structure	Propidium dye (Mahto, Chandra and Rhee, 2010) BrdU (Mahto, Chandra and Rhee, 2010) Ethidium homodimer (Mahto, Chandra and Rhee, 2 DAPI (Mahto, Chandra and Rhee, 2010) TUNEL assay (Reddivari *et al.*, 2007)
Total cellular protein	Sulforhodamine assay (Mahto, *et al* 2010)
Glucose	Fluorescent glucose analog (Leira *et al.*, 2002)
Intracellular Ca	Fluo 322 (Venkatesh *et al.*, 2004) Fluo 422 (Venkatesh *et al.*, 2004)
Lysosomal activity	Neutral Red assay (Reddivari *et al.*, 2007) Cathepsin D activity assay (Lee *et al.*, 2007) Granzyme based assay (Bird *et al.*, 2005)

Adopted from Jain AK, Singh D, Dubey K, Maurya R, Mittal S, Pandey AK. Models and Methods for *In vitro* Toxicity. In: *In vitro Toxicology*. Elsevier Inc.; 2018.

1.2.4 Drug Testing in Cancer:

Drug screening is a lengthy, tedious, and expensive process. It is estimated that only 5% of drugs entering clinical trials are approved by the Food and Drug administration (FDA). Moreover, a vast majority of the drugs that enter clinical trials proved out to be less efficient and effective in therapeutic aspects and most of the cancer remains untreated (Yakisich, *et al.* 2012). Ideally speaking drug testing should be a combination of speed, simple and low costs with optimal predictability of pharmacodynamics activity.

Broadly, preclinical screening of new drug can be classified as cell based screening assay which includes: a) Conventional cellular screens b) Tailored cellular screens c) Biochemical screening assay d) Combination of targets and cell screens e) Using model organisms for screening and cell free high throughput screening (HTS) on isolated targets. Cell free high HTS methods have several advantages like miniaturization, robot aided automatization and data management by novel management technologies over cell based screening (Lewis, 2012).

1.2.4.1 Review on drug toxicity testing in cancer:

A brief review of various tumor models proves that over a time, a transition have been observed from empirical drug screening of cytotoxic agents to target oriented drug screening with defined mechanism of action (Lewis, 2012).

In 1955, it was found the transplanted tumor and clinical activity gave better compound efficacy on screening than mammalian cell and bacterial culture. Thus, the National Cancer Institute (NCI) began large scale anticancer testing using mouse tumor model (Data,et al,1966; GOLDIN *et al.*, 1961). Following this, NCI introduced a new tumor panel incorporating transplantable solid human tumor models that represents the histological types of cancer. In 1982, NCI employed a new method of sequential process of progressive selection where a product was exposed with a progressively greater biological and pharmacologic challenge at each stage (Venditti, Wesley and Plowman, 1984). The agents found to be active in standard tumor panel was subjected to secondary screening that was drug oriented. Though many tumor panels were used no positive correlation between clinical – preclinical efficacy was observed (Lodhia *et al.*, 2015).

Another study model that widely used a human tumor *in vitro* cell line. This model has the potential to evaluate a large number of anticancer agents and a broader preclinical examination (Double, *et al.* 1989). Initially, the cell line panel incorporated 60 different human tumor cell lines of diverse types of cancer. To date, approximately 85,000 compounds have been tested in this panel whereby sulforhodamine B (SRB) assay is used to check its cell viability (Skehan *et al.*, 1990). Three endpoints like GI50 (concentration required to inhibit 50% of cells), total growth inhibition and LC50 (concentration required to kill 50% of cells) are used to determine compound activity and whether a compound will be considered for further evaluation (Holbeck, 2004).

Hollingshead and colleagues developed the Hollow Fiber Assay (HFA) designed to identify *in vivo* activity of potential anticancer compounds. It has been

proposed that the continued use of HFA will exploit its ability to define specific pharmaco-dynamic end points at this early stage in a drug's evaluation. Before the usage of HFA, each compound was examined in murine models and 3 stem cell human tumor xenografts model defined as most sensitive in vitro ('Contributions to Oncology Beiträge zur Onkologie', 2002). However, many compounds that showed promising results in stem cell xenograft models gave disappointing results when replicated in clinical studies. Since the disparity between the clinical and preclinical evaluation is yet unsolved an orthotopic model has been used. The orthotopic transplantation model better suggests the morphology and growth characteristics of clinical disease and hence can serve as a more clinically relevant tumor model for tumor site and metastasis(Fidler, Naito and Pathak, 1990). This model also attempts to target processes involved in angiogenesis. Despite the application of obvious advantages, the models is hindered by several limitations (Bibby, 2004).

Another model is an autochthonous tumor that includes spontaneously occurring tumors and induced tumor growth. The model better mimics the human tumor models than transplanted tumors (orthotopic/stem cells). Despite its advantageous properties like orthotopic growth, tumor histology and a route of metastasis, the autochthonous tumor model owns several limitations ('Contributions to Oncology Beiträge zur Onkologie', 2002).

Over the past 20 years, genetically engineered cancer models (GEM) has been extensively used to replicate the genetic and molecular alterations in human cancer and use it in novel therapeutic applications for better clinical responses. The first strain of genetically modified mice predisposed to cancer was

a transgenic mouse model whereby cellular or viral oncogenes were introduced into the mouse germ line. Many GEM studies with transgenic and knockout approach, progressively introducing mutations, etc. has been attempted (Karreth and Tuveson, 2009) (Szadvari, Krizanova and Babula, 2016). GEM model also possesses well validated drug targets and a preclinical model to test modern small molecular therapeutics (Weiss and Shannon, 2003).

Juan Sebastian Yakisich has reported an algorithm for pre-clinical screening of anticancer drugs effective against brain tumor. Brain tumor treatment is much more difficult owing to the blood brain barrier. The study integrated stem cell biology and novel concepts of anticancer drug screening to develop a 7 step algorithm as a guideline for its evaluation(Yakisich, 2012). The flexibility of the algorithm helps to determine an early need for clinical trials providing a useful tool for translational research in neuro-oncology.

Xulang Zhang, *et al.,* have developed an *in vitro* multicellular tumor spheroid model (MCTS) model using human breast cancer cells encapsulated in alginate poly lysine algine. The model was subjected to chemotherapeutic drugs preceding its culturing and characterization study. The model has shown to be a rapid and valid *in vitro* model to screen therapeutic drug with a feature to simulate *in vivo* 3D cell growth pattern (Zhang *et al.*, 2006).

1.2.4.2 Various approaches of drug discovery:

The conventional anticancer drug discovery and development focused on the cytotoxic agents. The drug discovery paradigms select compounds that had significant cytostatic or cytotoxic activity on tumour cell lines and caused tumour

regression in murine tumour allografts or xenografts. This conventional screening of anticancer agents geared towards the selection of cytotoxic drugs.

On the other hand, the molecularly targeted agents act by mechanisms that may not result in direct and significant toxicity. These agents act on the extra cellular, trans-membrane, or nonnuclear intracellular processes. For example, compounds like 5, 6-dimethylxanthenone-4-acetic acid (DMXAA) target developing tumour vasculature and have proved to cure cancer when combined with conventional cytotoxic agents (McKeage, 2008). The discovery of molecularly targeted agents has altered the preclinical and clinical screening paradigm not only because of the dose-response, dose-toxicity, and mechanisms but these agents are associated with pre-targeted mechanisms of action. However, most molecularly targeted agents do not proceed to advanced stages in human clinical trials due to either efficacy or toxicity concerns. Also, combinational therapy is of significant importance here the actions of target-based drugs are supplemented by other agents and where the target-based drugs may act as sensitizers to the cytotoxic agents. Example: P-glycoprotein (membrane efflux protein responsible for multi-drug resistance in several cases) inhibitors. The target based drug works based on the following mechanism by: a) Facilitating apoptosis b) Inhibiting metastasis c) Inhibiting Angiogenesis and d) by using antibodies against tumour specific agents.

The therapeutic activity and toxicity of cytotoxic drug that is derived from the molecular mechanism can be directly correlated to the dosage of the drug. The narrowing of the therapeutic window of these drugs along with the serious disease condition of the patients and inter-individual variation in drug response

and toxicity constitutes a significant challenge in their clinical development and use. Thus, the treatment of tumour has been individualised based on the tumour type, histology, and the disease state. Pharmacogenomics and metabolomics are two such emerging paradigms for the individualization of drug therapy.

Pharmacogenomics is the genotypic and phenotypic imprinting to identify the genes and proteins involved in the pharmacokinetics and pharmacodynamics of drug response or toxicity. This analysis aid to minimize inter individual variations and side effects in a dose- response. Usually, drug targets or drug metabolizing agent act as targets for such genotypic profiling. Cytochrome P450 enzyme is one such drug metabolizing agent (Van Schaik, 2005).

On the other hand, metabolomics involves the quantitative analyses of metabolites in a cell, tissue, or organism. It mainly involves two strategies – target analysis and metabolite profiling (Claudino *et al.*, 2007).

Hence, pharmacogenomics and metabolomics approach can help achieve individualization of drug therapy to optimally balance efficacy with toxicity and contribute to the success of clinical development of novel drug candidates.

In addition to these agents, drugs acting via indirect mechanisms like immune-modulators, chemo protective agents, multidrug resistance reversing agents, hormonal drugs, photosensitizers, analgesics, anti-emetics, and bone marrow growth factors can be used in the management of cancer.

1.2.5 Various 3D models:

Cancer cells propagated in a 3 dimensional culture system exhibiting physiologically relevant cell-cell and cell-matrix interactions, gene expression and signalling pathway profiles, heterogeneity and structural complexity that reflect *in vivo* tumours (Nath and Devi, 2016). Various pre-clinical models and bio fabrication techniques have been employed to recapitulate the tumour micro environment. Some major bio fabrication technique for cancer 3D models encompasses:

a) **Tumour spheroid** are 3D cellular aggregates of uniform or heterogeneous cell populations derived from tissue fragments mechanically or enzymatically partially digested (LaBarbera, Reid and Yoo, 2012). Agitation based techniques, liquid over lay, hanging drop method and microfluidic reactors are four major techniques used to induce cancer spheroids *in vitro* (Nunes *et al.*, 2019). Tumour spheroids have been considered a gold-standard for cancer 3D culture, as they allow for the recapitulation of important features of TME heterogeneity (Sutherland, 1988).

b) **Scaffold based approach:** This technique involves seeding or encapsulation of tumour/stromal cells in biomaterials that mimic the ECM of solid tissues (Ma, 2004). Both natural and synthetic material can be used to fabricate the scaffold (Nyga, Cheema and Loizidou, 2011).

c) **Microfluidics:** Microfluidics chip can be used as dynamic bioreactors for the culture of tissue spheroids or for the precise shaping of micro-engineered cell-embedding hydrogels (Hsiao *et al.*, 2009).

d) **3D bio printing**: 3DBP an emerging technique used to design heterogeneous culture platforms in which the spatial organization of different types of cells, tissue interface or ECM is controlled (Jung, Lee and Cho, 2016). In case of cancer study, this method allow the systematic investigation of cellular/ECM structure-related influences on tumour microenvironment. The model also allow control over the bio ink properties and different components can be chosen depending on the purpose of the study.

e) **Organoids:** Organoids are considered the more physiological 3D culture models. Long term organoid cultures have been established from different primary and metastatic cancer tissues and have been reported able to resemble the tissue they were derived from(Simian and Bissell, 2017).

f) ***Ex vivo* tissue slices:** It represents a promising technique which preserves tissue 3D architecture and pathway activity for short time. This system help in the screening of novel immunotherapy agents and in monitoring T-cells (Vaira *et al.*, 2010).

1.2.6 3D Bio printing:

Rapid prototyping or additive manufacturing which is also popularly known as 3D bio printing (3DBP) is an emerging technology that commingles multidisciplinary knowledge to manufacture products with desirable characteristics properties. The patent of 3D printing was given to Chuck Hull for the stereo lithography apparatus in 1986 (Gu *et al.*, 2015). However, in consecutive years numerous technologies of 3D printing like selective laser sintering and fused deposition modelling were granted patents. A blueprint of the

product that has to be designed is modelled using CAD (computer-aided design) that is attached to a 3D printer (Gross *et al.*, 2014). Following modelling, successive layers of materials are printed and supports are removed or dissolved to get the finished product. These products have proved their versatility for various medical applications such as prosthesis development, stomatology, artificial skin, drug development, etc (Dimitrov, Schreve and De Beer, 2006; Gu *et al.*, 2015).

Conventionally, three mainstream strategies are employed in 3D bio printing. (a) **Inkjet method** of 3DBP is a contactless printing technique that was first used in organ printing. Mainly 2 types of printing are used in this method (piezoelectric type and hot bubble type) (Xu *et al.*, 2005, 2013). (b) **Extruded biological method** of 3DBP uses different cross-linking agents by chemical, physical and photonic means (Klebe, 1988). (c) **3D laser BP method** is based on the principle of laser induced forward transfer. It uses high-energy laser pulse that is illuminated on the energy-absorbing layer and mainly consists of a laser source, target boss and receiving layer (Klebe, 1988).

1.2.6.1 Ideal Material Properties of Bio printing:

Bio-ink is the salient printing material used in 3D bio-printing and this colloidal material is analogous to the ink used in an office or home desktop printer. Unlike non-biological systems, 3D bio-printing encounters many complexities like the choice of a biocompatible material, type of cell, growth and differentiation factor and sensitivity of cells and tissues. Thus, it is not easy to fabricate the

functional component of a living system as it requires more than a mere spatial rearrangement of biomaterial, bio chemicals, and cells in a layered fashion.

To effectively replicate the biological and physical properties of a cell construct via 3D bio-printing, the system has to meet some important requirements. Few such criteria are (1) **Printability** – Various parameters like viscosity, surface tension, surface properties of printer nozzle and cross-linking ability play a significant role in maintaining the complex 3D structure of the construct and for printing material with desired spatial and temporal control. It has been reported that the material with low thermal conductivityand with the ability to cushion cells improves the cell viability (Hopp, 2012). (2) **Biocompatibility** – means that the implanted material should get along with the construct without generating any undesirable effects (Hersel, *et al.* 2003). (3) **Degradation kinetics and by-products** – The rate of degradation can be defined in terms of the cell's capacity to synthesis the extracellular matrix. Degradation products have to be non-toxic, readily metabolized and cleared from the body else it can affect the biocompatibility. The swelling can cause the absorption of fluid from the surrounding tissue and contractile properties of the material result in the closing of pores and vessels required for cell migration and nutrient delivery. (4) **Structural and Mechanical properties** – Choosing of material with desired mechanical features like shear thinning, permeability to oxygen, nutrients and metabolic waste and in situ gelations is appreciable as it facilitates a continued function of the construct (Talbot *et al.*, 2012). (5) **Material Biomimicry** – The biomimetic components should be selected based on desired functional, structural

and dynamic properties of the materials and its implication to substantiate the purpose of study.

1.2.6.2 Classification of Bio ink:

Bio ink can be categorized based on two approaches that are widely accepted in 3D bio printing. The first and most common process is the scaffold-based bio printing(Klebe, 1988). In the scaffold-based approach, the cells are loaded on the exogenous material and bio printed in 3D constructs. While, in the second process named scaffold-free bio printing, neo-tissues are formed mimicking embryonic development. This engineered neo tissue is then deposited in a specific pattern to fabricate a large scale functional tissue.

Hydrogel is a scaffold-based bio-ink with moisturizing and cross-linking properties caricaturing the extracellular matrix. It has excellent biocompatibility and biodegradability that makes it an appropriate candidate to stay in contact with the biological system for a considerable period. Various types of hydrogel – natural (like alginate, gelatin, hyaluronic acid, chitosan, collagen type 1, fibrin and agarose) and synthetic (like methyl acrylate gelation and Polyethylene glycol) are used in 3D bio printing. Each of these hydrogels has its own characteristics properties that aid to serve its specific purpose in 3D bio printing.

1.2.6.3 3D Bio Printing and Cancer Study:

3D bio printing (3DBP) that allow assembly of cells and extracellular matrix to form an *in vitro* cellular models for 3D biology research have proven its implication in a plethora of field. 3D models have aided to overcome the

limitations of conventional 2D models which has been shown via cell proliferation, morphology, gene expression, protein synthesis, and drug metabolism studies. The flexibility and biomimetic property of 3DBP construct has been used in the printing of large scale 3D tissue constructs (Yan *et al.*, 2005), *in vitro* liver tissue (R *et al.*, 2010), adipose tissue (Rui Yao *et al.*, 2009), bone tissue (Fedorovich *et al.*, 2008) and hybrid tissue constructs with vascular network (Shengjie Li *et al.*, 2009). 3D bio printed skin can serve as a skin substitute, used in cell therapy and wound healing (Velasquillo *et al.*, 2013).

For the past one decade use of the 3DBP technique in cancer studies have surged at a higher rate(Liu, Delavaux and Zhang, 2019). Xingliang Dai, *et al.,* have reported the use of 3D bio printed glioma stem cells to develop a brain tumour model to study its drug resistance. This 3D Alginate/Gelatin/Fibrinogen based glioma stem model has proved to be a novel alternative tool for studying gliomagenesis, glioma stem cell biology, drug resistance, and anticancer drug susceptibility invitro (Dai *et al.*, 2016).

Yu Zhao, *et al.,* have bio printed a cervical tumour model using HeLa cells in Alginate/Gelatin/Fibrinogen hydrogel. This 3D *in vitro* model showed about 90% cell viability and higher MMP expression and chemo resistance than in the 2D culture system. Thus, the work proved that studies like cell proliferation, drug metabolism, morphology, gene expression, and protein synthesis gave better results on 3D construct than using 2D models(Zhao *et al.*, 2014). Ying Wang, *et al.,* 3D bio-printed a breast cancer model for drug resistance study. The study involved co-culture of adipose derived mesenchymal stromal cells with human epidermal receptor 2 positive primary breast cancer cells in 2D and 3D culture and

their response to doxorubicin. The model proved to faithfully reproduce the *in vivo* condition and serve as a better model for cancer study and drug screening (Y. Wang *et al.*, 2018). Jorge, *et al.,* bioengineered breast cancer microenvironment via 3DBP. The study showed how biochemical factors like matrix associated proteins, soluble factors, and synthetic biomaterials can modulate ECM, using a bio printed construct. The cancer cell-ECM interaction can be used to understand relevant cancer specific architecture, stromal cell interaction, significant physiological signals, immune, and vascular components (Belgodere *et al.*, 2018).

3DBP can serve as an effective tool improving the *in vitro* model study of metastasis with heterogeneous tumour microenvironment (Albritton, *et al.* 2017). 3D models can also advent an eon of immune oncology by an assembly of T cells, cancer associated fibroblasts, and extracellular matrix (Di Modugno *et al.*, 2019).

1.2.6.4 Review on Lung Cancer Study Using 3DBP:

The study on lung cancer more specifically non-small cell lung cancer (NSCLC) using bioprinted *in vitro* model commenced in 2015 with Mou H, *et al.,* developing a 3D bioprinted agarose alginate scaffold cultured with NSCLC 95 D cells. The morphology, proliferation, and associated protein expression of lung cancer cells in 3D culture systems was distinctively compared with the 2D culture. This model was found to better mimic the *in vivo* lung cancer microenvironment and turned out to be a promising model for *in vitro* lung cancer study (H Mou *et al.*, 2015).

Laila C. Roudsari and her colleagues conducted a study (2017) on lung adenocarcinoma cell responses in a 3D *in vitro* angiogenesis model and correlated with its metastatic capacity. The study utilized a biomimetic modified synthetic hydrogel of Poly (ethylene) glycol with 3 types of lung cancer cells. The cells readily formed spheroid layer and also recruited vascular cells when cultured in a 3D hydrogel. However, a difference in the morphology, interactions between vessels invading the cancer layer, and the cancer cell structures were observed among these 3 cell types (Roudsari, *et al* 2018).

In 2018, Xiong Wang, *et al.,* bio fabricated a tumour like lung cancer model using A549 cell line with Sodium alginate/Gelation hydrogel. The lung cancer model was cultured for 28 days and it was found to maintain its structural integrity. Histology, gene analysis, and scratch test showed that the *in vitro* model was more biomimetic compared to 2D models, and it is highly valuable in biomedical research (X. Wang *et al.*, 2018).

Arindam Mondal, *et al.,* (2019) developed a Sodium Alginate – Gelatin hydrogel by optimising the rheological parameters to print the NSCLC patient derived xenograft (PDX) and lung cancer associated fibroblasts (CAF) co-culture. The study demonstrated that the rheological optimisation significantly enhanced the printability and viability of NSCLC PDX and CAF co-culture which allows 3D co-culture spheroid formation within the printed scaffold. Thus, the model can be used for studying high throughput drug screening and other preclinical applications.

1.2.6.5 Use of 3DBP in Drug Toxicity Testing of Cancer:

The preclinical screening for drugs is an unavoidable step that aids to prioritize the compound for its further development. This preclinical selection has reached an eon of target-driven molecular approach from its empirical screening. This target-oriented molecular approach which answers the drug-target cell interaction and its mechanisms has to carefully plan and validated. The drug screening strategy has been lately updated with a rational drug discovery model that combines the novel knowledge with the proteomics, genomics, and bioinformatics information. However, these drug screening fails to give expected results in clinical trials owing to its limitation to bio mimic the *in vivo* microenvironment and lack of control over the parameters in the culture system. Regarding the above review, it can be doubtlessly stated that 3DBP can serve as an efficient *in vitro* model for cancer pathogenic study and drug screening.

1.2.7 Composition of this Novel Bio ink system:

1.2.7.1 Sodium Alginate:

Alginate, also called algin or alginic acid is a natural polysaccharide derived from brown alga. It constitutes the second most abundant polysaccharide on earth derived seaweed (Tønnesen, *et al* 2002). Structurally, it comprises of β D mannuronate (M block) and β L guluronate (G block) bonded by 1, 4 linkage. The M and G block can be combined in different sequences or alternately combines with cations to ensure the binding of water molecules, drugs, and bioactive substances in 3D structure. The mechanical strength and degradation rate of alginate hydrogel is directly related to the G/M ratio. Higher the G/M ratio

creates a stiffer and slow dissolving hydrogel (Vanderhooft, Mann and Prestwich, 2007). Alginate has high carboxylic acid content that aids it to absorb a high amount of water.

Sodium alginate has Sodium attached to the carboxylic group which can be modulated with bivalent and trivalent cations such as Ca^{2+}, Ba^{2+}, Fe^{2+}, Mg^{2+} and Al^{3+} which add on to the mechanical strength of the hydrogel. The cross linking of these ions can create a soft and flexible hydrogel. Also, studies have shown that Ca^{2+} cross-linked to Sodium Alginate can enhance the proliferation and differentiation of *in vitro* osteoblasts.

Alginate is not degraded by mammalian cells as it lacks alginase but rather is degraded via replacement of divalent cations. It costs less, abundantly available, and shows good compatibility with minimum inflammatory response on *in vivo* implantation (Orive *et al.*, 2002). Because of its shape, fidelity, and volume retention *in vivo* (CM *et al.*, 2013) and *in vitro* (Cohen *et al.*, 2006) it can serve as a good hydrogel model in a plethora of tissue engineering fields. Applications of Sodium alginate have been mainly targeted at musculo-skeletal tissue such as cartilage(Cohen *et al.*, 2006), osteochondral interface (Fedorovich *et al.*, 2012) and bone (Fedorovich, et.al 2008; GS *et al.*, 2014). It is also used in a more specialized field of bio fabrication and 3D bio printing, such as wound healing, artificial skin, and drug delivery.

Some of the attractive features of alginate include biocompatibility, good printability, mild gelation condition, improved absorption capacity, mechanical stability, and viscoelastic properties and ability to form modified

alginate derivatives with new desirable properties, helps to widen the implication of alginate in the diverse field of medical sciences (Abasalizadeh *et al.*, 2020).

Studies have demonstrated that chemically modified alginate can be used as a carrier to enhance the efficacy of chemotherapeutic agents used in cancer therapy. For instance, the injectable hydrogel of Alginate-g-Poly (N-isopropylacrylamide) has been used for sustained release and effective delivery of anti-cancer drugs, doxorubicin overcoming the multidrug resistance in prostate cancer treatment (Liu *et al.*, 2017). Another example is lectin-conjugated chitosan–Ca–Alginate in microparticle form which is used to deliver the drug molecules, 5-Fluorouracil to colon region, and improve the efficacy in targeted anticancer colon drug therapy (Glavas-Dodov *et al.*, 2013).

1.2.7.2 Gelatin:

Gelatin is a water soluble biodegradable polypeptide derived by partial hydrolysis of collagen, which is a fibrous protein found in the connective tissue within the human body. Several types of gelatin exist with different compositions depending on the source of collagen and the hydrolytic treatment method. For instance, mammalian derived gelatin from pig or bovine, widely used in regenerative medicine over the past one decade have polypeptide structure that resembles a human being and this gelatin differs significantly from fish derived gelatin (Hulmes, 2002).

Irrespective of its origin, gelatin typically compose of Glycine-X-Y peptide triplets repetitions. X for proline and Y for hydroxyproline are the most common formulations(Foox and Zilberman, 2015). However, the amino acid

composition and its sequences vary depending on its origin and this results in variation in its properties.

Gelatin is a mixture of about 20 amino acids is connected by a peptide bond. Also, the average length and molecular weight of gelatin depend on the origin of the raw material, pretreatment methods, and hydrolytic parameters (like temperature, pH, and time). Between these individual gelatin chains there exist strong non-covalent interactions like van der Waals forces, hydrogen bond, electrostatic and hydrophobic interactions. Also, the immunogenicity of gelatin is significantly lower than its progenitor Collagen 1 owing to the degradation of propeptides and triple helix structure(Karim, *et al* 2009).

Gelatin solution exhibits an amphoteric behaviour due to the presence of alkaline amino acid and acid functional groups. It is a water soluble natural polymer that absorbs 5 to 10 times the equivalent weight of water. Another unique property of gelatin is the ability to be gelled at a low temperature of 20-30^{0}C by cooling them to form a hydrogel. This is referred to as sol-gel transition or gelation. During this process, the locally ordered regions of gelatin are joined by non-specific bonds (such as hydrogen bond, electrostatic and hydrophobic bonds). The resultant hydrogel owes a thermo-reversible character i.e. they are thermo-responsive since the non-specific bond can be easily broken down via heat. Thus, the thermo-sensitive property of the gelatin solution bestows good printability to gelatin based hydrogel used in 3DBP (Wang *et al.*, 2017).

1.2.7.3 DEAE Cellulose:

Diethyl Aminoethyl (DEAE) Cellulose is a weak anion exchanger used extensively in ion-exchange chromatography to segregate positively charged

proteins or nucleic acid into the matrix. Structurally, it composes of the DEAE chain that is covalently attached to the oxygen atom on the D-glucose subunit of cellulose.

S. Reuveny, *et al.,* have demonstrated that DEAE cellulose anion exchangers can be used as a cheap and easy-to-handle micro-carrier for culturing several anchorage dependent cells. Smith, et al in 1982 have demonstrated the DEAE cellulose ability for cell attachment and capacity to support growth of anchorage dependent cells. DEAE cellulose particles also support growth of establishes cell lines like IBHK and MDCK to full confluency (Smith, 1982).

Another study by Ramin Ramezani Kalmera, *et al.,* have fabricated and evaluated carboxymethylated diethylaminoethyl cellulose micro carriers as support for cellular applications. So far studies proven cellulose based micro carrier enhances cell adhesion and proliferation. However to facilitate cell attachment to their surface, they require an appropriate functional surface charge. Cell functions such as growth and adhesion can improve by modifying the molecule with a cationic and anionic group. Thus carboxymethylated diethylaminoethyl cellulose (CM-DEAEC) was produced by ionic crosslinking. The findings showed that CM-DEAEC micro carriers support cellular attachment and proliferation very well and hence are promising materials for cell therapy and tissue engineering applications (Ramezani Kalmer *et al.*, 2019).

Since various studies have indicated that DEAE cellulose can improve cell adhesion and proliferation, it can be used as a hydrogel component in 3DBP for effective anchorage and growth of cells.

1.2.7.4 Collagen Peptide:

Collagen is the most abundant extracellular fibrous protein that is known for its biomedical application due to its excellent biocompatible and biochemical features. However, recent studies have shown that smaller molecular weight collagen i.e. collagen peptide owes several intrinsic potencies than its progenitor collagen.

Collagen peptides are short chain protein building blocks synthesized by hydrolysis of native collagen. Depending on the applied enzymatic process of hydrolysis, a characteristic pattern of collagenic fragment is generated that demonstrates its distinct features. Collagen peptides are relatively small molecules with molecular weight less than 10,000 g/mol. The peptide comprises of at least 2 amino acids or at most 100 amino acids. Due to its high buffer capacity, collagen peptide in liquid guarantee pH stability on exposure to an acid or base. Like any other protein, collagen peptide has an isoelectric point between 5 - 6 that ease it's to combination with other proteins. Collagen peptide has been tested for degradation rate and has found to be stable both quantitatively and qualitatively.

Over 90% protein content of the molecule makes it an ideal candidate for protein fortification and therapeutic food. It also forms an important element of healthy nutrition as it promotes the growth of bone, joints, muscles, and skin. They are easily soluble in cold water, heat stable, and non-allergic. Unlike gelatin, it does not form gel even in high concentration.

Also, studies have proved that collagen peptides to promote cellular growth. Paresh A, *et al.,* have used collagen-mimetic peptide modifiable hydrogels for articular cartilage regeneration. The work involved modification of Streptococcal

collagen-like to develop a hydrogel system. The hydrogel was encapsulated with human mesenchymal stem that substantially improved the viability and Thus, the work highlighted the use of this novel biomaterial to modulate cell-mediated processes and create functional tissue engineered constructs for regenerative medicine applications(Parmar *et al.*, 2015).

Xiaoxiao Wen, *et al.,* demonstrated immobilisation of collagen peptide (Col-p) on dialdehyde bacterial cellulose (DBC) nanofibers via covalent bonds for tissue regeneration. Cell study indicated that the prepared DBC/Col-p composite was bioactive and suitable for cell adhesion and attachment. The work indicated that the composite is a promising material for tissue engineering and regeneration(Wen *et al.*, 2015).

Jeevithan Elango, *et al.,* have proved that collagen peptide up regulates osteoblastogenesis from bone marrow mesenchymal stem cells through MAPK-Runx2. The study involve the extraction of collagen peptide from Mahi mahi fish (Coryphaena hippurus) bones and test its osteogenic potential using bone marrow mesenchymal stem (BMMS) cells. This study concluded that collagen peptide from Mahi mahi bones possess excellent osteogenic properties and could be used for bone therapeutic application(Elango *et al.*, 2019).

1.2.8 Gap Area:

It is not surprising that the rapid attrition in drug development observed over the past two decades has alarmed the need for an effective preclinical drug testing system. The emergence and advancements in 3D bio printing have aided to compensate many setbacks of the conventional 2D models and thereby

accurate fabrication of an efficient drug screening model. Though numerous studies have been initiated to develop an ideal bio ink formulation several limitations pertaining to the work persist. Thus, developing an ideal bio-ink to overcome the existing limitation is the need of hour. The study on development and evaluation of a 3D bio-printed construct for drug screening and an obvious application in cancer therapy holds significance.

1.2.9 Advantages of the proposed bio ink system:

Bio ink has been widely used in 3D bio printing to homogeneously encapsulate cells and other bioactive materials. Various formulations of bio-inks are studied and optimized for better printability, degradation, and cell-material interaction but the challenge remains to develop an ideal bio ink with adequate bio mimicking nature.

Bapi Saker. *et al.,* have reported that Alginate Dialdehyde (ADA) - Gelatin based hydrogel can effectively encapsulate the cells. Although this system efficiently satisfies various favourable properties of a hydrogel like hydrophilic nature, biocompatibility, ease of gelation, and controlled degradation. It lacks cell adhesion and the variation in pH during ADA -Gelatin synthesis can also affect the cell viability (Sarker *et al.*, 2014). Another study has demonstrated that the mechanical and cell adhesion property of Gelatin – Sodium Alginate hydrogel can be controlled by varying the concentration of each of these components and thereby can tailor material with desired mechanical and physiological properties (Mondal *et al.*, 2019). Numerous studies have been initiated the limitation of these hydrogel system demands replacement with an ideal bio ink. Hence, we propose

a novel bio ink formulation using Sodium Alginate crosslinked with Calcium ions, amine rich gelatin, Diethyl Aminoethyl (DEAE) cellulose, and Collagen Peptide.

Sodium Alginate a natural polymer with excellent biocompatibility, has been widely used as a hydrogel component. It also has sheer thinning or thixotropic property i.e. the viscosity decreases on sheer strain. However, lack of cellular adhesion and control over its visco-elasticity property have delimited its usage in 3D bio printing. Gelatin that is a collagen-derived compound with distinct gelation property, can be used in combination with Sodium Alginate to improve the printability of 3D structure. Also, this blend of Sodium Alginate-Gelatin can increase the thermal stability of gelatin and delay in gelatin exudation from the bio fabricated scaffolds at 37 °C (Giuseppe *et al.*, 2018). The cytocompatibity of Sodium Alginate can be improved using Gelatin because of the presence of tripeptide arginine–glycine–aspartic acid (RGD Sequence) which is originally described as cell binding motif present in fibroblasts (Sarker *et al.*, 2017). Studies has proved that there is strong interaction between sodium alginate and gelatin molecules resulted from intermolecular hydrogen bonds and ionic interactions (Xiao *et al.*, 2001). Also, crosslinking of Sodium Alginate with Calcium chloride gives a stiffer scaffold via ionic interaction of carboxyl group of Sodium Alginate with Calcium ions.

Cell adhesion property can be improvised using Collagen Peptide and DEAE Cellulose. DEAE cellulose is a weak anion exchanger used extensively in ion-exchange chromatography. The positively charged DEAE group can bind with the negative charge of the cell membrane and carboxylic acid of alginate

enhancing the cell adherence property (Ramezani Kalmer *et al.*, 2019). Collagen peptides that are short-chain protein building blocks synthesized by hydrolysis of native collagen have been proved to increase cell proliferation and cell adhesion property due to the interaction of arginine-glycine-aspartic acid (RGD) sequence with the integrin protein present on the cell surface (Hersel, Dahmen and Kessler, 2003). The structural stability and longevity of the bio ink in 3D gel structure have also been elevated by the presence of DEAE cellulose and Calcium ions in the dispersion medium.

The stability of the hydrogel can be ensured using DEAE Cellulose that degrades at a much lower rate than other component of hydrogel. Thus, DEAE cellulose enhance the mechanical strength and degradation kinetics of the scaffold. As each hydrogel component are biopolymers it generates a non-toxic by product on gradual degradation of the scaffold this add on the longevity and structural integrity of hydrogel.

1.2.10 Hypothesis:

The study proposes fabrication of hybrid bio ink (AGDCelCp) formulation using Sodium Alginate cross-linked with Calcium ions, Gelatin, Diethyl Amino ethyl (DEAE) Cellulose, and Collagen Peptide. The development of 3D bio-printed cancer tissue model using this novel bio ink for drug testing application.

1.2.11 Objectives:

In order to validate the hypothesis specific objectives were defined as mentioned below

1. Optimization of the bio ink formulation
2. Optimization of printability
3. Fabrication of 3D bio printed construct
4. Characterization of the construct
5. Cytotoxicity Assay
6. Evaluation of 3D printed construct
7. Preliminary Drug testing of the 3D construct

Chapter 2

2.1 Materials:

DMEM/F-12 (Hyclone - Dulbecco's Modified Essential/Ham's F-12 Medium, USA), FBS (Gibco, Brazil), 100X antibiotics (Gibco, USA), trypsin (Gibco, USA), Collagen Peptide (Nitta Gelatin, India), Sodium azide, Propidium Iodide, Hematoxylin Solution, Eosin. MTT Reagent, DEAE Cellulose, Gelatin, Sodium Alginate, Alamar blue and Mitoxantrone dihydrochloride (all of these materials were procured from Sigma Aldrich, USA).

2.2 Methodology:

2.2.1 Cell culture:

A549 cells and L929 cells were cultured in DMEM/F 12 (Hyclone - Dulbecco's Modified Essential/Ham's F-12 Medium, USA) with 10% FBS (Gibco, USA) and 1X antibiotics (Gibco, USA) in a 5% CO2 incubator at 37ºC. The cells were sub cultured using 0.25% trypsin (Gibco, USA). The media was changed the next day and then was changed every alternate day.

2.2.2 Optimization of Bio ink Formulation:

The concentration of collagen peptide used in the bioink was optimised using L929 (fibroblasts cell line) and A549 (lung cancer cell line) cells. Collagen Peptide (Nitta Gelatin, India) solutions were prepared in different dilutions

(5 µg/ml, 10 µg/ml, 20 µg/ml, 50 µg/ml and 100 µg/ml) in DMEM-F12 media. A549 cells and L929 cells were seeded in a 96 well plate at a density of 25,000 cells/cm^2 and 15,000 cells/cm^2, respectively and cultured in DMEM-F12 media. After 24 hours of culture, media was discarded and 200 µl media with collagen peptide of various concentrations were added, media without collagen peptide was added to control wells. The next day, following removal of the media, 50 ul of MTT reagent [Sigma Aldrich] (1 mg/ml) was added and incubated for 3 hours. The reagent was discarded and well was rinsed with 100% Isopropanol. Absorbance was read at 595nm using an automated microplate reader and cell viability was calculated. The concentration of collagen peptide was thus, fixed and 2% Sodium alginate [Sigma Aldrich, USA], and 3.33% Gelatin [Sigma Aldrich, USA] was chosen based on the concentration used in the previous studies standardized in the laboratory. In order to fix the concentration of DEAE cellulose a degradation study was carried out as follows.

It was found that the printed construct degraded at a faster rate when the concentration of DEAE Cellulose was varied above 1% and below 0.5%. Thus, the degradation study of the bioink was performed for 5 days in PBS (Phosphate Buffer Saline) at various concentrations of DEAE Cellulose [Sigma, USA] (0.5%, 0.8% and 1%). The constituents of bio ink involve 2% Sodium alginate, 3.33% Gelatin, 20 µg/ml collagen peptide, and DEAE Cellulose varying its concentration in each construct (n=3). The construct was visually observed for its degradation and stability, images of the bio ink were taken till Day 5.

2.2.3 Characterization:

2.2.3.1 Swelling Study:

The physical characterization of the 3D printed construct (AGDCelCp) was performed using swelling and degradation study.

2% Sodium Alginate was prepared in HBSS buffer by keeping it overnight, stir the gel at 200 rpm for 5 minutes at 40^0 Celsius. Following the dissolution of sodium alginate and collagen peptide at a final concentration of20 µg/ml was added. Stirred it at 200 rpm for 5 minutes and then add 0.5%, 0.8%, and 1% DEAE cellulose to each set of the construct (n=3), stir it well. Later on, Gelatin was added at a final concentration of 3.33% and stirred it for 2 minutes at 200 rpm. Printed the gel after loading it in a syringe as described earlier. The bio-ink was printed in 6 layers and the volume of each layer was 66.6 µl.

The construct was incubated in DMEM F12 media (with 10% FBS, 1X antibiotics, and 0.04% sodium azide). The reading of the swollen construct was taken at regular intervals of 2 hours. The reading was taken until the sample showed maximum swelling. The samples were then kept at -80^0C overnight and lyophilized for 6 hours. The lyophilized constructs were then used for degradation study.

The swelling index and water uptake of the construct were calculated using the following formula:

Swelling Index = $[(S_w - D_w)/D_w] \times 100$

Water Uptake = $[(S_w - D_w)/S_w] \times 100$

Where S_w indicates the weight of swollen gel and

D_w indicate the weight of the dry gel

2.2.3.2 Degradation study:

After the weight of the lyophilized sample was taken at 12th hour (W_{max}). The constructs (with 0.5%, 0.8% and 1% DEAE Cellulose) were incubated in DMEM media (with 10% FBS, 1x antibiotics, and 0.04% sodium azide). The reading of the degradation study was taken after day 1, day 3, and day 7 after lyophilizing the sample (n=3). The percentage of degradation was calculated using the formula:

$$\textbf{\% Degradation} = (S_w/W_{max}) \times 100$$

Where S_w indicates the weight of gel at regular intervals

W_{max} indicates maximum swelling at 12th hour.

2.2.3.3 Fourier Transform Infrared (FTIR) Spectrometer:

The chemical characterization of the bioink and the presence of each component of bio-ink was studied using FTIR [Nicolet 5700, Thermo Fischer]. The bioink was prepared as per the above- mentioned protocol and lyophilized after freezing it overnight. Likewise, each component of the bioink system in its powdered form was lyophilized. Attenuated total reflectance Fourier transform infrared (ATR-FTIR) spectra of the samples were recorded at a wavelength of 0 cm^{-1} – 4000 cm^{-1}.

2.2.3.4 Micro Computed Tomography (MicroCT):

The average pore size of the bioink was characterized using Micro CT [Micro CT 40, Scanco Medical, Switzerland]. The bioink was prepared and cast in a petri dish. The sample was then lyophilized and it was given to study the

porosity of the bioink formulation. The porosity of the sample was calculated using the below-stated formula:

Porosity = [1 - (Material Volume/Total Volume)] x 100

2.2.3.5 Scanning Electron Microscope (SEM):

The surface topography of the bioink was investigated using a scanning electron microscope. The bioink was fabricated as per the above-stated protocol. Following lyophilization, the sample was placed on double-sided tape, sputter-coated with gold, and examined under SEM [Hitachi, Model S- 2400, Japan]. The images were acquired at different magnifications (800X, 200X, and 400X).

2.2.4 Cytotoxicity Testing:

The cyto-compatibility of bio ink formulation (AGDCelCp) was evaluated using direct contact and test on Extract.

2.2.4.1 Direct Contact:

An in vitro cytotoxicity test using direct contact method was performed using (AGelDCelCp) sample as per ISO 10993-5. In the Direct contact assay, Ultra High Molecular Weight Poly Ethylene (UHMWPE) was used as negative control and stabilised PVC disc was used as positive control. L929 cells were cultured and test samples, negative controls and positive controls were placed on the cells. After incubation at 37°C for 24 h, cell morphology was studied microscopically to study its reactivity around the sample. The reactivity was graded as 0, 1, 2, 3 and 4 as per the table given below:

Grade	Reactivity	Description of reactivity zone
0	None	No detectable zone around or under specimen
1	Slight	Some malformed or degenerated cells under specimen
2	Mild	Zone limited to area under specimen
3	Moderate	Zone extending specimen size up to 0.33 cm
4	Severe	Zone extending farther than 0.33 cm beyond specimen

2.2.4.2 Test on Extract:

Test on extract was studied based on MTT assay. Extract was prepared by incubating the test samples (AGDCelCp) with culture medium containing serum at 37º C for 24 hour**.** The extract was diluted with culture medium to get 100%, 50 %, 25% and 12.5%. Cells cultured in normal medium was considered as cell control. Ultra High Molecular Weight Poly Ethylene (UHMWPE) was chosen as negative control and diluted phenol positive control.

Equal volume of various dilution of test samples, extract of negative control, cell control and positive control were placed on L-929 cells. After incubation of cells, extract and control medium was replaced with 50µl MTT solution and were incubated at 37°C for 2 hours. After discarding the MTT solution, 100 µl of Isopropanol was added to all wells. The absorbance was read at 570 nm using a spectrophotometer. The cell viability was calculated using the below mentioned formula: **Percentage viability = (Absorbance of Test/Absorbance of control) *100**

2.2.5 Development of 3D Bio-printed Tissue Construct:

A standard CAD design previously developed in the laboratory was used for printing the bio-printed construct. Briefly, the CAD design was formulated using Repetier Host software for fabrication of a 6 layered or 3 stacked cylinder-shaped structure with total height of 2460 um and diameter of 1.5 cm. The CAD design was saved as stl.file. Later the stl.file was converted to G-code and then 3D bio-printed construct was developed using Cell Ink Inkerdible 3D bio printer.

The 3D bio-printed construct was developed as follow. Sodium Alginate (0.06 g) was dissolved in 2 ml of Hank's Balance Salt Solution (HBSS) by keeping it overnight. Thus, the concentration of Sodium Alginate in the final bioink will be 2%. The sodium Alginate solution was stirred at 220 rpm for 2 minutes and 60 µl of collagen peptide was added to get a final concentration of 20 µg/ml and stirred at 220 rpm for 2 minutes. Later, DEAE cellulose was added to get a final concentration of 0.8% and stirred for at 220 rpm for 3 minutes. The total volume was adjusted up to 3 ml by adding Gelatin solution at a final concentration of 3.33% and stirred at 200 rpm for 2 minutes. The cells were resuspended in gelatin solution for bioprinting. The bioink (AGDCelCp) was printed using Cell Ink Inkredible printer at flow rate of 10 mm/second, the pressure of 120 kPa, and a nozzle diameter of 410 µm. 3D bioprinting was also carried out using Regen HU 3D Discovery printer. Following printing, the gel was cross-linked using 2 ml of 0.1M Calcium chloride solution and the solution was discarded after two minutes.

2.2.6 Evaluation of 3D Printed Construct:

2.2.6.1 Live Dead Assay:

The construct with a cell density of 3 million cells/ml was printed and cultured. Fluorescein Diacetate (FDA) stock at a concentration of 10 mg/ml was prepared in acetone and a working solution was made by adding 10 µl of FDA stock in 1ml of serum-free media. Propidium Iodide (PI) stock of 1 mg/ml was prepared in ethanol and a working solution was made by diluting it in 1ml of HBSS buffer. FDA was added on the construct for 2 minutes and discarded. After a wash with HBSS buffer, PI was added and incubated for 30 seconds. The assay was performed on Day 0, 1 and 2 and was the images were captured using an inverted fluorescent microscope [Leica DM IRB].

2.2.6.2 H-E staining:

The 3D printed construct was fixed with 10% Neutral Formaldehyde buffer (NBF) for 15 minutes at room temperature and wash with MilliQ water. The samples were cut into thin slices by cryo-section. A few drops of Hematoxylin solution were added on the slices and incubated for 2 minutes at room temperature. After a wash with MilliQ water and 75% ethanol. Given again a MilliQ wash and added eosin stain on the slices for 30 seconds. Excess stain was removed with filter paper. The test sample was observed under a microscope and imaged.

2.2.6.3 MTT Assay:

The 3D printed construct (n=3) with A549 cell with density of 3 million cells/ml was cultured in DMEM- F12 media and MTT assay was performed on Day 0,1 and Day 2. The culture media was discarded and MTT reagent (0.5 mg/ml) was added and incubated for 4 hours. Following the removal of the MTT reagent hydrogel sample was incubated with Acidified Isopropanol for 30 minutes. Absorbance was read at 595 nm using an automated microplate reader and cell viability was calculated.

2.2.7 Evaluation of 3D Bio printed construct for Drug Testing:

3D bio printed cancer tissue model was developed using A549 cells as described earlier. For this study cells cultured in standard culture well (2D) were used as a positive control. The cells in 2D culture system (25,000 cells/cm^2 in 96 well plate) and 3D bio printed construct were initially cultured in DMEM F12 media for 24 hours The media was discarded after 24 hours and Mitoxantrone was added at a concentration of 2 μM, 4 μM, 8 μM and 10 μM to both 2D and 3D models and the cell viability was calculated using MTT assay as described earlier for Day 1 and Day 3.

2.2.8 Statistical Analysis:

For each test at least three replicate samples were examined and Average $\pm$ Standard Deviation was calculated. Statistical significance was determined using Student's T test. P value less than 0.05 was considered as statistically significant.

Chapter 3

3. Results:

3.1 Optimization of Bio ink system:

The concentration of Collagen Peptide used in this bio-ink system was fixed based on MTT assay. The cell viability of L929 (fibroblast cell line) and A549 (lung cancer cell line) was assessed following the culturing of cells for 24 hours in a 96 well plate at a seeding density of 15,000 cells/cm^2 and 25,000 cells/cm^2 respectively. Post culturing in DMEM- F12, the media was discarded and Collagen peptide was added at a various concentration (5 µg/ml, 10 µg/ml, 20 µg/ml, 50 µg/ml and 100 µg/ml) to the 2D culture system. MTT assay was performed after 24 and 48 hours. L929 cells and A549 cells in Collagen Peptide showed significantly higher percentage viability for Day 1 and Day 2 at 20 µg/ml (clearly depicted in Figure 1 and Figure 2). Thus, a concentration of 20 µg/ml collagen peptide was chosen for bio-ink formulation. The concentration of DEAE cellulose was chosen via a degradation study for 5 days in PBS. Different 3D bio-printed constructs (n=3) was made using various DEAE cellulose concentration (0.5%, 0.8%, and 1%), 2% Sodium Alginate, 3.33% Gelatin and 20 µg/ml of collagen peptide. The constructs were visually observed and it was found that construct with 0.8% DEAE cellulose retained its integrity even after Day 5 implying better longevity and stability than other constructs (at 0.5% and 1% DEAE Cellulose) (Fig 3). The construct with 1% DEAE Cellulose degraded much faster and so couldn't image on 5^{th} day.

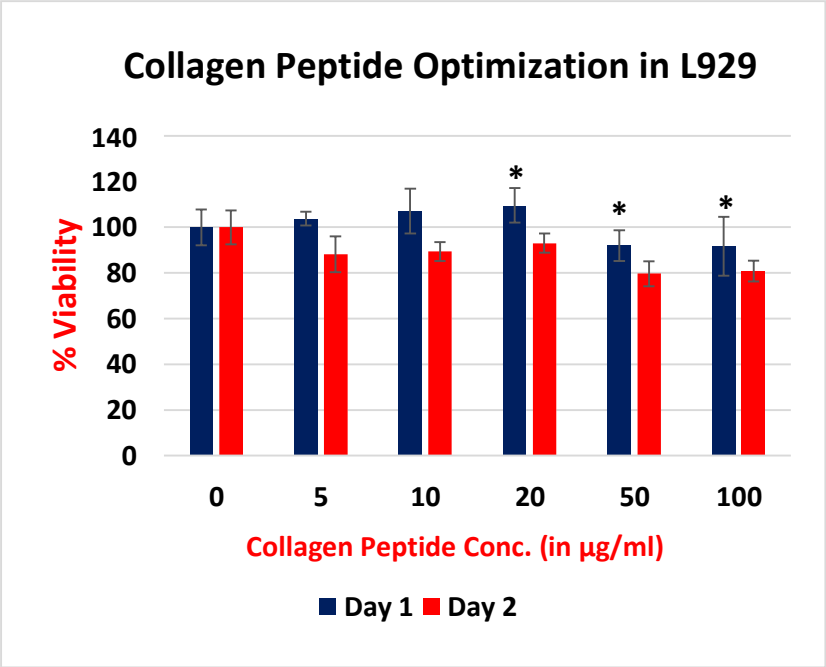

Figure 1: Depicts the difference in cell viability of L929 cells after culturing in various concentration of collagen peptide for 24 and 48 hours (*p<0.05).

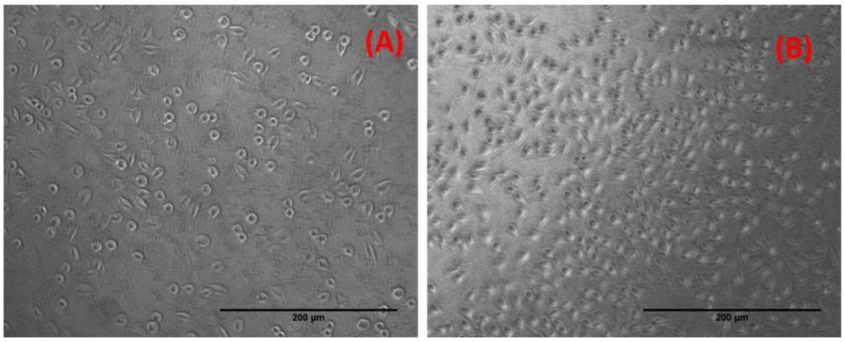

Figure 2: Depicts microscopic images (under magnification of 10X) of Collagen Peptide Optimization in L929 cells after 24 hours. Image A and B represents Control and L929 cells with 20 µg/ml concentration of collagen peptide,

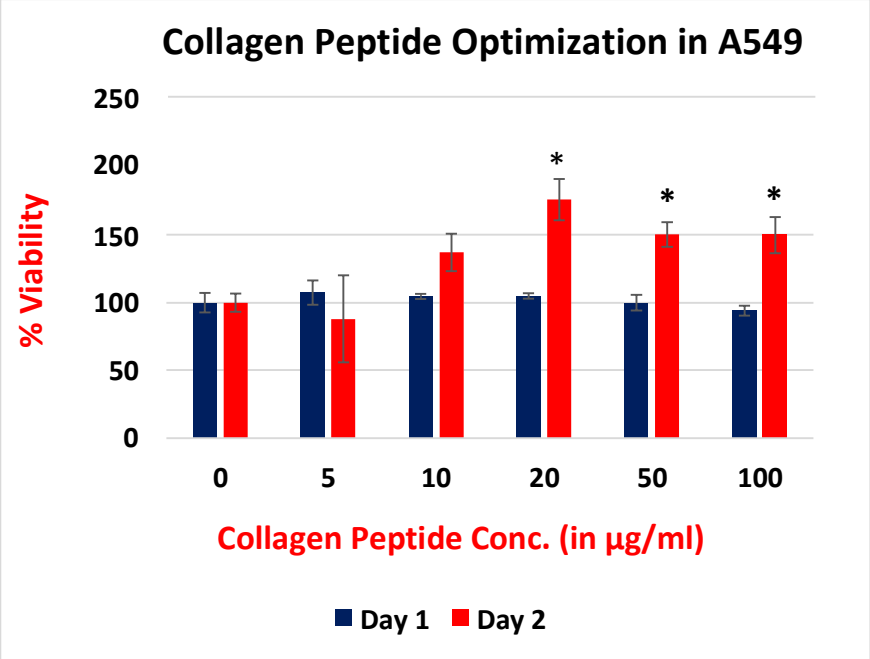

Figure 3: Depicts the difference in cell viability of A549 cells on Day 1 and Day 2 at various concentration of collagen peptide

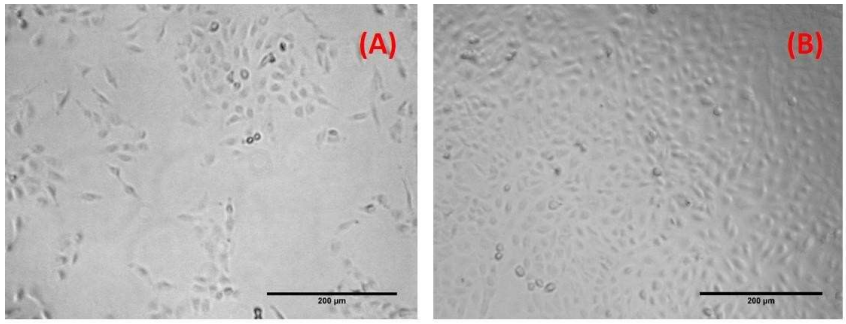

Figure 4: Microscopic images (under magnification of 10X) of Collagen Peptide Optimization in A549 cells after 24 hours. Image A and B represents Control and A549 cells with 20 µg/ml concentration of collagen peptide, respectively.

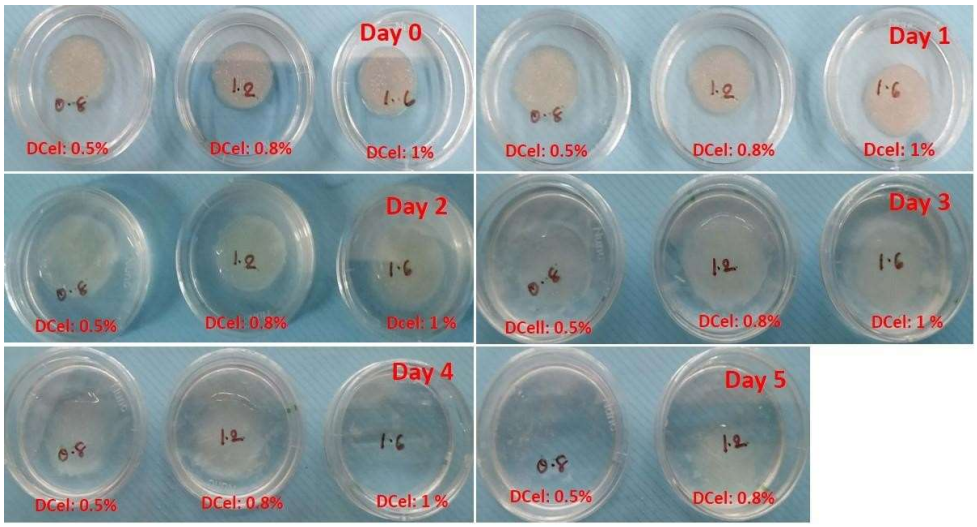

Figure 5: Images of the degradation study in PBS illustrates that the bio ink formulation with different concentration of DEAE Cellulose (DCel).

3.2 Characterization:

3.2.1 Swelling:

The 3D printed construct was fabricated using the bio-ink (AGDCelCp). Each set of construct (n=3) with different concentration of DEAE cellulose (0.5%, 0.8%, and 1%) was evaluated for its swelling characteristics.

It was found that all three sets of the construct (with 0.5%, 0.8%, and 1% DEAE cellulose) showed swelling index in the range of 1400 (Fig 6). However, as the construct reaches its maximum swelling in 12th hour 0.5% and 0.8% showed higher and similar swelling index throughout the study period when compared to 1%.

The water uptake capacity of the construct in various DEAE Cellulose concentration was also evaluated. All three concentrations of DEAE cellulose did not show any significant difference in its water uptake value (Fig 7).

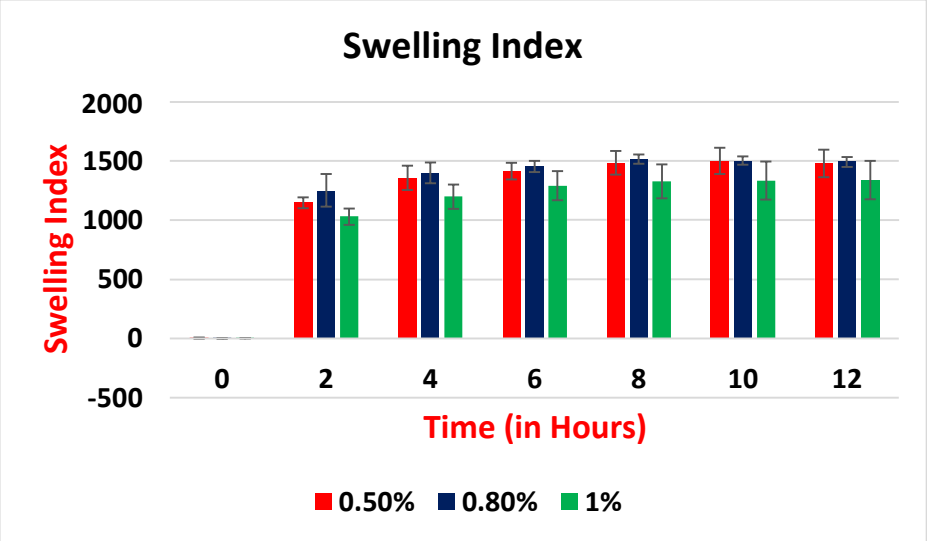

Figure 6: Depicts the swelling capacity of construct with different DEAE cellulose concentration (0.5%, 0.8% and 1%).

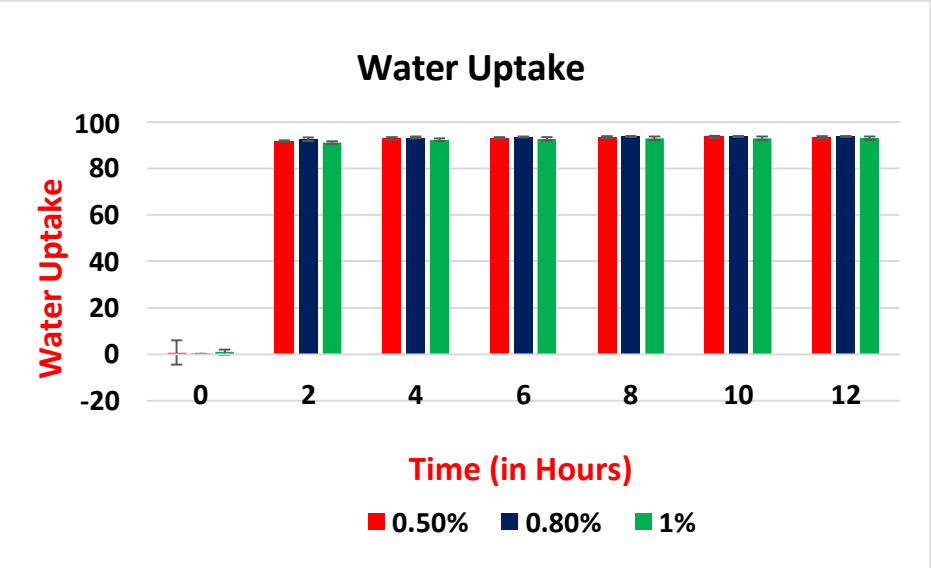

Figure 7: Illustrates the water uptake capacity of each construct with various DEAE cellulose concentration of 0.5%, 0.8% and 1%.

3.2.2 Degradation:

Following the swelling study, the constructs were frozen at -80^{0}C and lyophilized. The dry weight of the samples was taken at its maximum swelling (12th hour) and the degradation study was conducted in DMEM F12 media with 10% FBS, 1x antibiotics, and 0.04% sodium azide. The degradation was calculated based on the percentage of weight loss. The samples were lyophilized and dry weights were taken after incubating the constructs for 24 hours (Day 1), 72 hours (Day 3), and 168 hours (Day 7). On day 7, construct with 0.8% DEAE cellulose showed comparatively lesser residual weight loss when compared to other concentrations (Fig 8 and 9). The construct with 0.8% DEAE cellulose was found have better handling property. All the constructs were found to be stable in culture media even upto 7 days. Based on the stability observed in culture media and also in PBS the construct with 0.8% DEAE cellulose was selected as the optimum. Thus, the bio-ink composition was set as 2% Sodium Alginate, 3.33% Gelatin, 0.8% DEAE Cellulose and 20 μg/ml of Collagen peptide.

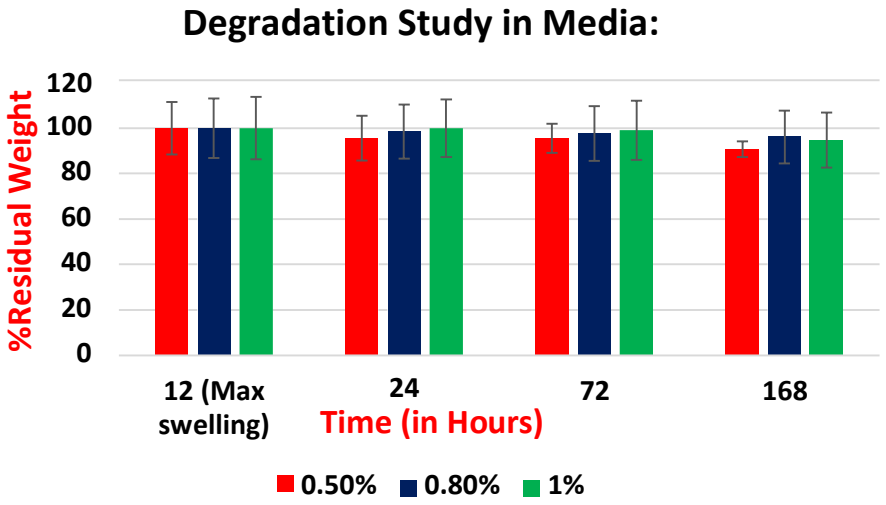

Figure 8: Depicts graphical representation of 3D printed construct with different DEAE Cellulose concentration in DMEM F12 media.

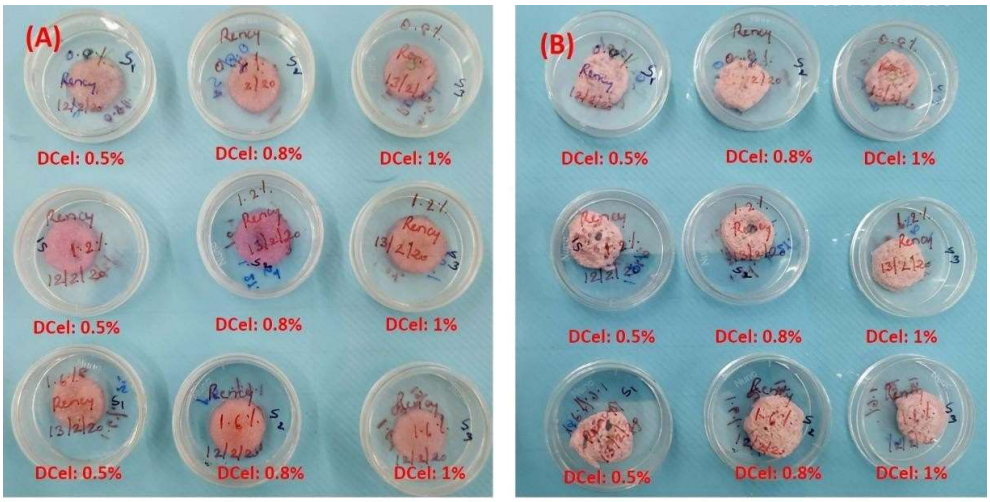

Figure 9: Images represent the degradation study of the 3D printed construct with various DEAE Cellulose (DCel) concentration in media.

3.2.3 Fourier Transform Infrared (FTIR) Spectrometer:

The bioink (AGDCelCp) were lyophilized and given for FTIR analysis along with the bio-ink components (Sodium Alginate, Gelatin, DEAE Cellulose, and Collagen Peptide) in powdered form. The reading was taken in the wavelength range of 0-4000 cm^{-1}. Sodium Alginate exhibited characteristics peak at 3231, 1593, 1404, and 1025 cm^{-1} corresponding to hydroxyl, asymmetric carboxyl group, symmetric carboxyl group, and ether, respectively. The Gelatin showed band position at 3303, 1633, 1546, 1451, and 1239 cm^{-1} of hydrogen bond water and amide A/NH stretching, amide I, amide II, symmetric and asymmetric bending vibrations of the methyl group and amide III. DEAE Cellulose showed the band at positions 3329, 1313, 1157, and 1025 cm^{-1} relating to the hydroxyl group, -CH group in glucose unit, ether group, and β-glycosidic linkages. In the case of Collagen Peptide, the characteristic spectrum was observed at 3237,1634,1525,1445 and 1238 cm^{-1} indicating Amide A, Amide I, Amide II, the vibration of collagen type 1 and Amide III, respectively.

The bioink showed an absorption spectrum at 3286, 1636, 1549, 1408, and 1031 cm^{-1}. The absorption spectrum at 3286 cm^{-1} indicates the stretching vibration of the O-H bond. The normal band position of the O-H bond is normally found in the wavelength of 3700-3100 cm^{-1}. As a result of N-H bending and C-H stretching, the Amide II band position was observed at 1549 cm^{-1}. Also, due to the electrostatic interaction between the carboxyl group of Sodium Alginate and an amino group of Gelatin, the characteristic absorption bands of the carboxylate group of Sodium Alginate at 1593 and 1404 cm^{-1} shifted towards higher wavenumber at 1636 and 1408 cm^{-1}, respectively. Another band

was exhibited at 1031 cm^{-1} position signifying the presence of ether group (–C–O–C pyranose ring skeletal vibration) from DEAE Cellulose. Thus, the characteristics absorption spectrum of each component was found on the FTIR spectrum of final product, AGDCelCp (Figure 10).

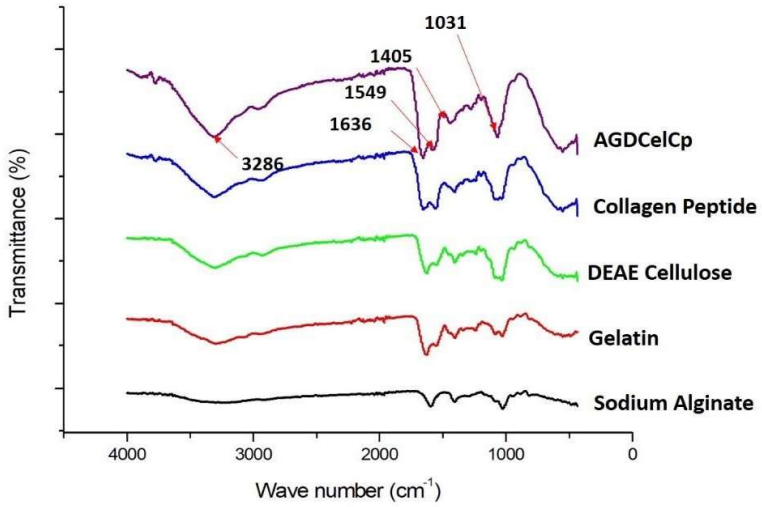

Figure 10: Depicts the FTIR spectrum of AGDCelCp and its components

3.2.4 Micro Computed Tomography (Micro CT):

The bio ink formulation (AGDCelCp) was prepared, lyophilized, and Micro CT analysis was carried out. Micro CT data shows that the average porosity of the bio ink formulation is 85% (Fig 11), indicating that the scaffold is porous enough to allow cell growth and diffusion of water and nutrient.

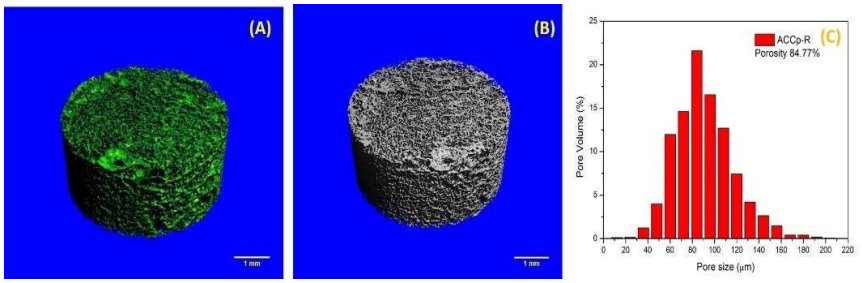

Figure 11: Image A and B represents the MicroCT images of the bioink while Image C shows the average porosity evaluated using MicroCT.

3.2.5 Scanning Electron Microscopy (SEM):

The bioink (in casted form) was lyophilized and imaged using SEM. The images were taken with 200X, 400X, and 800X magnification. It can thus, be interpreted from the images that the scaffold is porous with an average pore size of 73 um (in 400X magnification) (Fig 12).

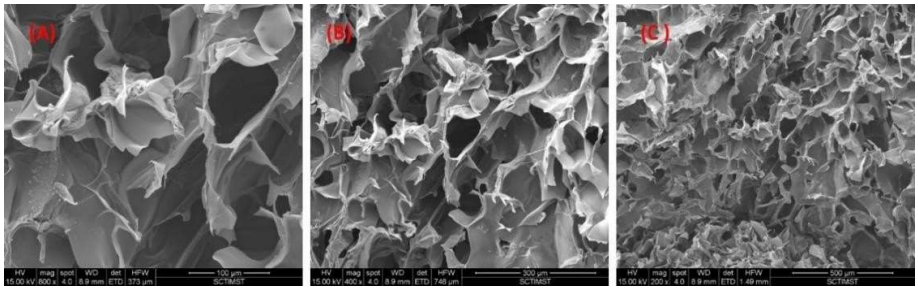

Figure 12: The SEM image depicting the porous structure of the bioink at magnification of 800X (Image A), 400X (Image B), and 200X (Image C).

3.3 Cytotoxicity Testing:

The cyto-compatability evaluation of the AGDCelCp bio-ink was studied using Direct Contact and Test on Extract. The following results were obtained:

3.3.1 Direct Contact:

The cytotoxicity reactivity of test and control samples were evaluated under an inverted phase-contrast microscope as per the table mentioned in the methodology.

Sl No	Sample	Grade	Reactivity
1.	Negative Control	0	None
2.	Positive Control	4	Severe
3.	AGDCelCp	0	None

As per ISO 10993-5, the achievement of a numerical grade more than 2 is considered as a cytotoxic effect. Since the test material, AGDCelCp achieved a numerical grade not greater than 2, the materials are considered as non-cytotoxic. Negative control gave none cytotoxic reactivity and positive control gave severe cytotoxic reactivity as expected (Fig 13).

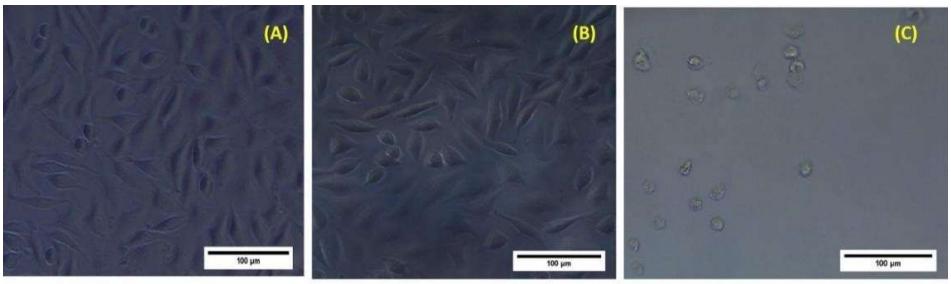

Figure 13: Depicts the direct contact results of the AGDCelCp under magnification of 20X. Images A, B and C shows the morphologic view of AGDCelCp, negative control and positive control, respectively.

3.3.2 Test on Extract:

The MTT assay of L929 cells after 24h contact with 100%, 50%, 25% and 12.5% AGDCelCp showed 87.25%, 90.24%, 95.72% and105.17% while negative control showed 98.86% and positive control showed 11.32% metabolic activity, respectively (Fig 14). Since AGDCelCp results showed cell viability above 60% on testing it clearly implies that the biomaterial is non-cytotoxic (Fig 14).

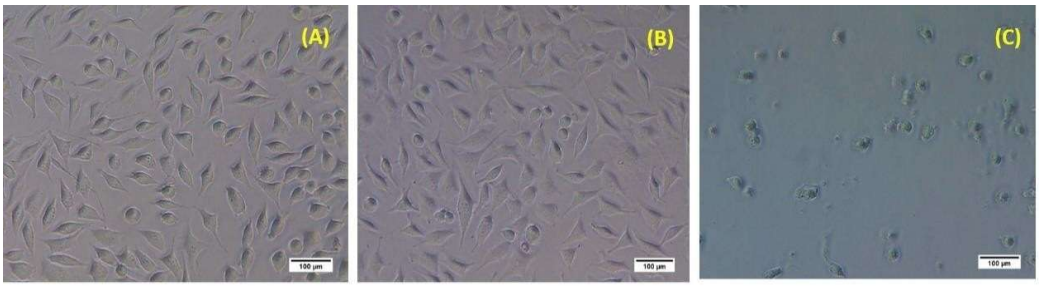

Figure 14: Represents the microscopic view of test on extract study of AGDCelCp under 20X magnification. The image A, B and C shows the morphologic view of AGDCelCp, negative control and positive control, respectively.

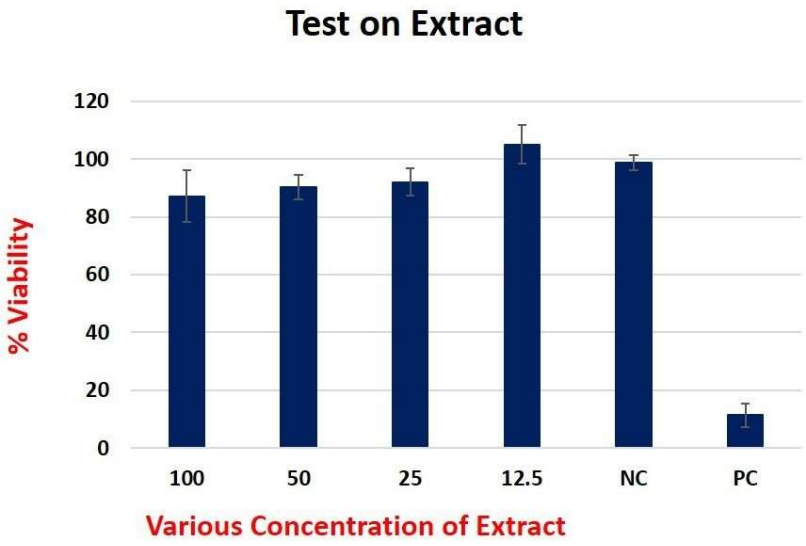

Figure 15: A graphically representation of test on extract evaluation of AGDCelCp, positive and negative control.

3.4 Printing Parameters:

The printing parameters were set at flow rate of 10 mm/second, the pressure of 120 kPa, and a nozzle diameter of 410 µm as per the previous work carried out in the laboratory. The 3D bio-printed construct was developed using the parameter and printed as per the CAD design.

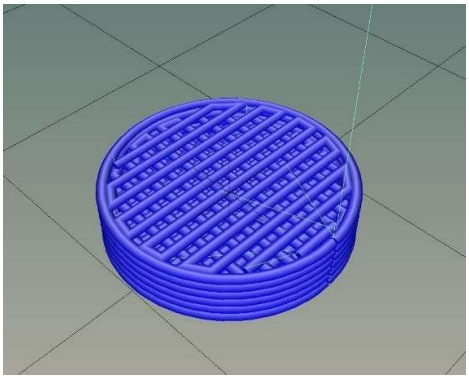

Dimensions of CAD design:

Number of layers: 6
Number of stacks: 3
Height of each layer: 410 µm
Total Thickness: 2460 µm
Diameter: 1.5 cm

Figure 16: Represent CAD design of 3D bio-printed construct and beside it is table detailing its dimensions.

3.5 Development of 3D bio-printed construct:

3D bio printed construct was fabricated with cell density of 3 million cells/ml and was cultured in DMEM-F12 media. Given below (Fig 17) are photographs of 3D bio-printed construct printed in three stacks and cultured for 24 hours in DMEM F12 media.

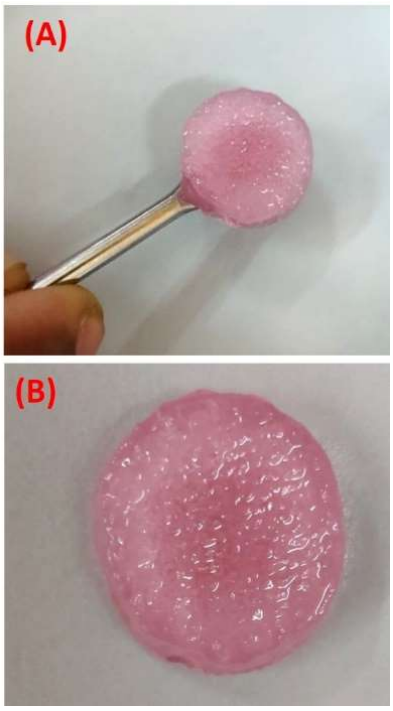

Figure 17: Image A and B are the digital images of multi-stacked 3D bio-printed construct after 24 hours culturing in DMEM F12 media.

3.6 Evaluation of 3D printed construct:

3.6.1 Live Dead Assay:

FDA-PI study was conducted on Day 0, Day 1 and Day 2 of the 3D bio-printed construct with A549. Live cells and dead cells are stained by FDA and PI,

respectively. It was observed that the bio ink supported the survival and the growth of cells as the construct had stained FDA throughout, and only very few PI stained cells were observed on all days of analysis (Fig 18).

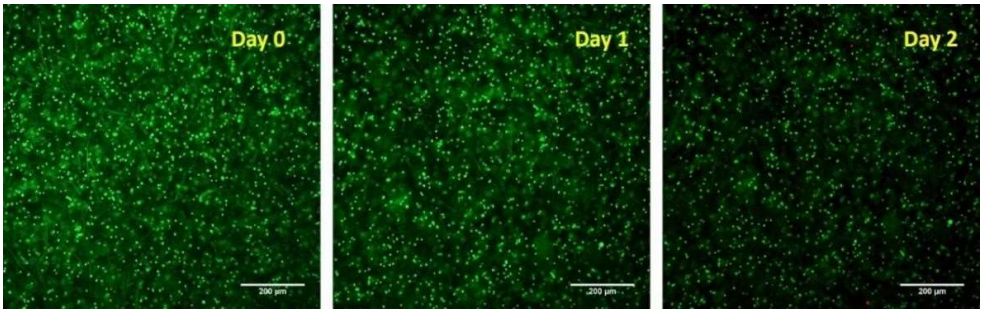

Figure 18: Illustrates live dead assay using FDA-PI staining. A549 encapsulated 3D printed construct was observed under fluorescent microscope (magnification of 10X) on Day 0, Day 1 and Day 2.

3.6.2 H-E staining:

Histological evaluation was performed to identify the uniform distribution of cells to the core of the 3D bio-printed construct using Hematoxylin Eosin staining. The 3D printed construct with A549 cells was cultured in DMEM F12 media for 5 Days, cryo-section were taken and evaluated after Hematoxylin Eosin staining. Images were taken under phase contrast inverted microscope under 10X and 4X magnification and it was found that A549 cells were distributed uniformly throughout the printed construct (Fig 19). The pink round structure represents the cells while the stained fibrous structure observed was the DEAE cellulose that remains non-degraded in the construct giving it mechanical strength and helps in the uniform distribution of the cells.

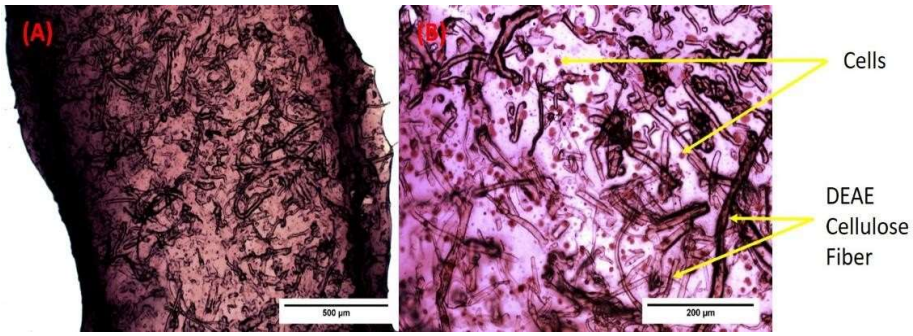

Figure 19: Images depicts the H-E stained 3D printed construct with A549 cells on Day 3, observed under magnification of 4X (Image A) and 10X (Image B) in an inverted phase contrast microscope. In Image B, the round- pink stained and fiber like structure represents the uniformly distributed cells and non-degraded DEAE cellulose, respectively.

3.6.3 MTT Assay:

The quantitative data supporting the cellular growth and its proliferation was achieved using MTT. MTT assay of the 3D bio printed construct was performed on Day 0, Day 1 and Day 2. The results clearly depicts that cell number is doubled when compared with day 0. The results of day 2 also suggests that cells continued to proliferate and survived in the construct (Fig 20). The percentage viability on day 1 and 2 shows significant difference (p value < 0.05) with reference to day 0 and this has been determined using T test.

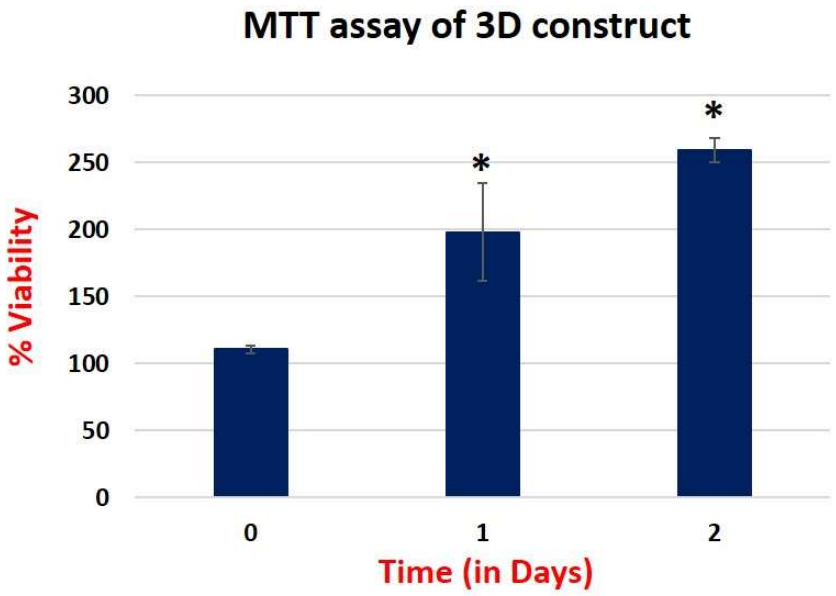

Figure 20: Graph represents percentage viability of 3D printed construct with A549 cells on Day 0, 1 and 2 (*p<0.05).

3.7 Proof of concept evaluation of 3D bio printed construct as a drug testing model:

The drug testing potential of the 3D bio printed construct was studied using Mitoxantrone (an established anticancer drug) after 24 hours of culture of the bio printed construct in DMEM F12 media. The cells cultured on tissue culture wells (2D) were used as positive control. After treating the system with different concentration of drugs (2 µM, 4 µM, 8 µM and 10 µM) the cell viability was calculated using MTT assay on Day 1 and Day3. It was found that on 2D culture system and 3D printed models drug Mitoxantrone reduced the viability significantly but at different rates. The drug, showed higher effect on A549 cell on Day 3 in both systems (Fig 21 and 22) The percentage viability also showed difference in both system but the pattern of toxicity was found to be similar on

both system. The higher toxicity in 2D system may be due to the difference initial cell number in both systems.

The results depict that 3D bio-printed structure successfully replicates the drug testing already proven in 2D culture system.

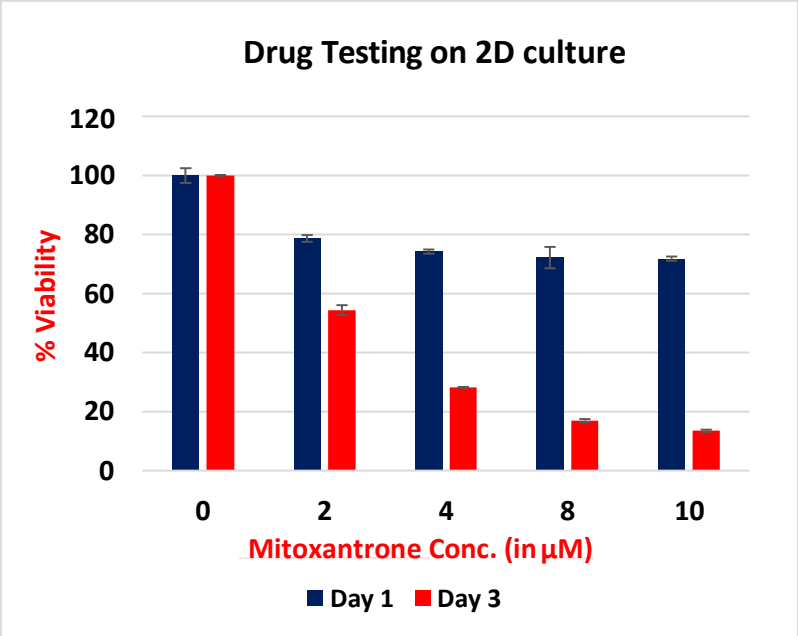

Figure 21: The graph illustrates the decrease in cell viability on drug treated 2D culture system

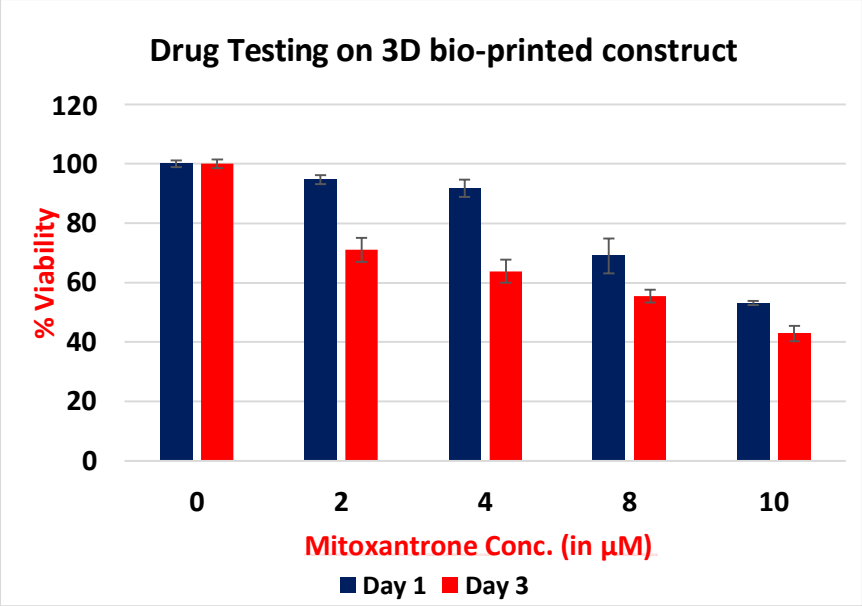

Figure 22: Graph depicting the decrease in cell viability of drug treated 3D bio-printed construct.

Chapter 4

4.1 Discussion:

Over the mid-twentieth century, the advent of *in vitro assay* has substituted the *in vivo studies*, triggering a drastic change in the paradigm of cytological evaluation. Since then numerous in vitro models ranging from the conventional 2D culture system to the trending 3D models have been greatly explored. The core reason for the wide acceptance of the 3D models is due to its ability to mimic the physiological microenvironment. Other features that make it superior over the 2D culture system involves the Cell – Extracellular matrix (ECM) interaction, flexibility to introduce desired biochemical factors thereby altering cellular behaviour (Belgodere *et al.*, 2018). However, the scope of these 3D models has been widened by the emergence of 3D bio printing technology.

3D bio printing (3DBP) gives access to structurally well-defined objects, with the possibility to create complex and heterogeneous structures, achieving a wide range of biological and mechanical properties to effectively encapsulate the cells in the biomaterial in the desired pattern (Valot *et al.*, 2019). Though various formulation of the bio ink with excellent printability, desired degradation kinetics, biocompatibility, and mechanical strength has been widely explored yet the challenge remains to develop an ideal bio-ink with adequate bio mimicking nature.

The current study endeavors to optimize and fabricate a bio ink formulation with Sodium Alginate, Gelatin, DEAE (Diethyl Aminoethyl) Cellulose, and Collagen Peptide. Each of these components has been chosen as it

releases no cytotoxic products on degradation and also provide biomimetic cues in the bioink. Studies have proven that the combination of Sodium Alginate with Gelatin to exhibit excellent biocompatibility and can be used as a potential bio printable materials (Zhao *et al.*, 2014)(Mondal *et al.*, 2019). Çelik, E., Bayram have demonstrated that Calcium cross-linked Alginate does not affect the biocompatibility and cell viability (Çelik *et al.*, 2016). Thus, Sodium alginate cross-linked with Calcium Chloride was used in this hybrid bio ink system with other components thereby resulting in the formation of a mesh-like structure resembling ECM via electrostatic interaction. The ionic interaction mainly involves in this hybrid system is owing to the binding of Sodium Alginate to Gelatin, crosslinking of Calcium with Sodium Alginate, and binding of DEAE (positively charged) with the cell membrane and carboxyl group of alginate (both of these are negatively charged). The cell adhesion property of the bio ink is expected to improve due to the presence of Collagen peptide (Parmar *et al.*, 2015; Elango *et al.*, 2019). Also, the structural stability and longevity of the bio ink in 3D gel structure are expected to elevate by the presence of DEAE cellulose and Calcium ions in the dispersion medium. Thus, the study expects the outcome of an optimized bio ink with good printability, degradation property, and cell viability.

In this study, we evaluated the suitability of developing a novel bioink consisting of Sodium Alginate, Gelatin, DEAE cellulose and Collagen Peptides. This bioink was characterized and evaluated for its suitability in developing a 3D bioprinted cancer tissue construct using A549 cells for anticancer drug testing. This bioink can be used for developing any tissue model. At present study, we

exemplify the fabrication of 3D printed lung cancer tissue. 3D printed lung cancer tissue construct is developed via encapsulation of A549, non-small cell lung cancer (NSCLC) cell line. The study holds significance in the current scenario owing to the high malignancy rate of NSCLC and the lack of an efficient drug screening model.

The study commenced with the optimization of the bio-ink system. The concentration of bio-ink components was chosen mainly based on its ability to give optimal printability, biomimetic cues and degradation kinetics. The concentration of Sodium Alginate and Gelatin was fixed at 2% and 3.33%, respectively based on previous literature (Mondal *et al.*, 2019) and initial studies carried out in the lab. The concentration of Collagen peptide was fixed via the following study in which, A549 cells and L929 cells were cultured and treated with Collagen peptide at different concentration of 5 µg/ml, 10 µg/ml, 20 µg/ml, 50 µg/ml and 100 µg/ml for 24 and 48 hours. MTT assay was performed on Day 1 and Day 2 and it was found that the Collagen peptide showed significantly higher cell viability at 20 ug/ml when compared to other concentrations on both the cell lines studied. There was a significant difference in cell viability of A549 cells and L929 cells as the doubling time of these cells are different. A lowering of cell viability of both cell lines was observed on Day 2, a plausible reason for this could be the contact inhibition due to lack of space in 96 well plate for the proliferation of cells.

It was found that the printed construct degraded at a much faster rate when the concentration of DEAE Cellulose was varied above 1% and below 0.5%, respectively. Therefore, to optimize the concentration of

DEAE Cellulose, 3D printed construct was fabricated with varying DEAE Cellulose concentration (0.5%, 0.8%, and 1%). The degradation study of the constructs was performed for 5 consecutive days in PBS and it was visually examined. The study showed that construct with 2% Sodium Alginate, 3.33% Gelatin, 0.8% DEAE Cellulose and 20 µg/ml of Collagen Peptide showed higher longevity and stability than other constructs (with 0.5% and 1% DEAE Cellulose concentration).

3D bio printed construct was developed using nozzle diameter of 410 µm at a flow rate of 10 mm/seconds and pressure of 120 kPa. After the 3D printed construct was fabricated, the characterization of these constructs was performed. The physical characterization of the 3D construct was done using swelling and degradation study. As the degradation study performed in PBS for optimizing the DEAE Cellulose concentration did not give any quantitative data due to its poor stability in PBS. Interestingly the construct showed much higher stability and handling properties in culture medium containing Foetal bovine serum. Since the construct is meant to use in culture media, degradation studies is repeated with culture media for finalizing the optimum concentration of DEAE cellulose in the bio ink formulation. 3D bio printed construct (n=3) with different DEAE Cellulose concentration (0.5%, 0.8% and 1%) was subjected to both swelling and degradation study.

The swelling study was performed (in DMEM media containing FBS) till the 3D printed construct reached its maximum swelling (in 12th hour) and it was found that 0.5% and 0.8% showed closer swelling index values and water uptake value for at all three concentration of DEAE Cellulose did not show much

difference. The hydrophilic nature of the bio ink system can be inferred from the data. Comparatively lesser swelling index in 1% cellulose may be due to higher concentration of DEAE cellulose.

As a continuation of swelling study, degradation study was performed in DMEM F12 media with 10% FBS) and weight of the samples was taken each day (Day 1, Day 3 and Day 7) after lyophilisation. Degradation study was performed in media to replicate the actual culturing environment of a 3D printed construct. The degradation was calculated as % weight loss and it was found that constructs with DEAE Cellulose concentration of 0.8% showed lower percentage weight loss when compared to 0.5% and 1% on Day 7 thus, proving that the construct is more stable at DEAE cellulose concentration of 0.8%. Since stability and the handling properties of the construct with 0.8% DEAE cellulose was found to be superior in both culture media and in PBS. This concentration was selected for development of 3D bio printed tissue construct.

The chemical characterization of the bioink was performed using Fourier Transform Infrared (FTIR) Spectrometer. The final bioink formulation along with the individual component of the bio ink was subjected to spectral analysis. The presence of the characteristic absorption peak of individual components of the bio ink can be interpreted from the spectrum of the bioink formulation. The bioink formulation exhibited band at position of 3286, 1636, 1549, 1408, and 1031 cm^{-1}. The absorption spectrum at 3286 cm^{-1} signifies the presence of the hydroxyl group implying the hydrophilic nature of the bioink formulation (Daemi and Barikani, 2012). This band position is a common characteristic peak found vividly in all four bio ink components. The absorption

peak at 1636 and 1408 indicate a band shift due to electrostatic interaction of Sodium alginate and Gelatin (Xiao *et al.*, 2001; Sarker *et al.*, 2017; Giuseppe *et al.*, 2018). The band position at 1549 cm^{-1} depicts Amide 11 of Collagen Peptide (Sanden *et al.*, 2019) while 1031 cm^{-1} signifies the presence ether group of DEAE Cellulose (Ramezani Kalmer *et al.*, 2019). Thus, FTIR results recapitulate the presence of Sodium Alginate, Gelatin, Collagen Peptide, and DEAE Cellulose in the bio ink system. The morphological characterization of the bioink was performed using Micro CT and SEM imaging. The Micro CT showed average porosity around 85% thus proving that the bioink is porous to support efficient diffusion of water and required nutrients for cell survival. SEM images taken at different magnification affirms the porous structure of the bioink.

The cytotoxicity evaluation of the sterile bio ink was performed using MTT assay (direct contact and test on extract) as per ISO 10993-5. The sample (AGDCelCp) and its control were evaluated and were graded based on its morphological features. The results showed 0 grading for sample and negative control and grading of 4 for positive control. As per ISO 10993-5, the achievement of a numerical grade more than 2 is considered as a cytotoxic effect. Since our sample gave a grade of 0 it can be clearly stated as non-cytotoxic.

Test on extract was performed using MTT assay of various concentrations of the sample (AGDCelCp) extract along with positive and negative control. The MTT assay of L929 cells after 24h contact with 100%, 50%, 25% and 12.5% AGDCelCp extract showed 87.25%, 90.24%, 95.72% and 105.17% cell viability. The negative control showed 98.86% and positive control showed 11.32% metabolic activity, respectively. As AGDCelCp results showed

cell viability above 60% on testing it implies that the biomaterial is non-cytotoxic. The microscopic images of the sample, negative and positive control replicated the above stated MTT results.

The evaluation of the 3D bio-printed construct was performed both qualitatively and quantitatively. The qualitative evaluation was done using live dead assay and Hematoxylin Eosin (H-E) staining while the quantitative assessment was performed using MTT assay.

The results of the MTT assay and live dead assay of 3D bio printed structure on Day 0, 1, and 2 suggests that bio ink supported the survival and proliferation of A549 cells. The H-E staining on the cross-section ofthe cultured 3D printed construct suggests that the cells are uniformly distributed and survived in the depth of the construct. The microscopic images indicated cross sectional structure of the 3D printed construct proving uniform distribution of the A549 cells throughout the construct.

Following qualitative assay, MTT Assay were performed on Day 0, 1, and 2 on the bio printed tissue construct. Both the qualitative and quantitative assay proved the survival and proliferation of cells in the construct. The biological cues in the scaffold might have helped in the survival and proliferation of cells in the scaffold.

The proof of concept to evaluate use the developed 3D bio-printed cancer tissue construct as an anti-cancer drug testing model, a preliminary study was carried out using Mitoxantrone. Mitoxantrone, an established anti-cancer drug has been used for the study (Pawlik *et al.*, 2016). A549 cells were cultured in 2D and 3D system for 24 hours and were treated with Mitoxantrone at a

concentration of 2 μM, 4 μM, 8 μM, and 10 μM following MTT assay on Day 1 and Day 3. It was found that cell viability significantly reduced on Day 3 when compared to Day 1 on all concentrations of Mitoxantrone. Similar observation was observed in the experiment conducted in standard tissue culture dishes. The considerable lowering of cell viability on Day 3 proves that drug shows its optimal activity on day 3 when compared to Day 1 in the developed 3D construct, thus affirming the work of Pawlik.et.al on 2D culture system (2016). Thus, it can be inferred from the results that 3D printed structure successfully replicates the drug testing already proven in the 2D culture system. However, further study has to be performed to assess the efficiency and significance of a 3D bio-printed construct over the 2D model with multiple anticancer drug available for treatment.

4.2 Conclusion:

There is a need of biomimetic 3D models for *in vitro* drug testing. The usage of 3D bio-printed model can mimic the physiological micro environment via better cell-cell and cell-ECM interaction. Though various formulation of the bio ink has been widely explored for developing 3D tissue models, yet the challenge remains to develop an ideal bio-ink with adequate bio mimicking nature. Current study focused on the optimization, fabrication, characterization of an *in vitro* 3D bio-printed tissue construct followed by its evaluation, and a proof of concept drug testing. It can be inferred from the study that the bio ink system composed of Sodium Alginate, Gelatin, DEAE (Diethyl Aminoethyl) Cellulose, and Collagen Peptide used in the 3D model exhibited excellent printability, biocompatibility, cell viability and controlled degradation rate. Following the fabrication, evaluation and proof of concept validation of the 3D bio printed model was performed using Mitoxantrone (an established anti-cancer drug).

More follow up studies have to be carried out for the validation of the 3D construct as anticancer drug screening model. For instance, the rheological analysis could be done to substantiate the study with quantitative data to prove the strength of the bio ink and its shear thinning property. Also, studies using different drugs and various types of in vitro assays like Apoptosis assay, Tunnel assay, Caspase Assay, etc. has to been done to validate its efficacy. This proof of concept study opens up an avenue for the development of more reliable 3D bio printed drug screening system to replace conventional screening using 2D cell cultures and time consuming *in vivo* studies.

4.3 References:

Abasalizadeh, F. *et al.* (2020) 'Alginate-based hydrogels as drug delivery vehicles in cancer treatment and their applications in wound dressing and 3D bioprinting', *Journal of Biological Engineering*. BioMed Central Ltd., pp. 1–22. doi: 10.1186/s13036-020-0227-7.

Albritton, J. L. *et al* (2017) '3D bioprinting: Improving in vitro models of metastasis with heterogeneous tumor microenvironments', *DMM Disease Models and Mechanisms*, 10(1), pp. 3–14. doi: 10.1242/dmm.025049.

Belgodere, J. A. *et al.* (2018) 'Engineering breast cancer microenvironments and 3D bioprinting', *Frontiers in Bioengineering and Biotechnology*, 6(MAY). doi: 10.3389/fbioe.2018.00066.

Bibby, M. C. (2004) 'Orthotopic models of cancer for preclinical drug evaluation: Advantages and disadvantages', *European Journal of Cancer*. Elsevier Ltd, 40(6), pp. 852–857. doi: 10.1016/j.ejca.2003.11.021.

Bird, C. H. *et al.* (2005) 'Cationic sites on granzyme B contribute to cytotoxicity by promoting its uptake into target cells.', *Molecular and cellular biology*, 25(17), pp. 7854–67. doi: 10.1128/MCB.25.17.7854-7867.2005.

Çelik, E. *et al.* (2016) 'The effect of calcium chloride concentration on alginate/Fmoc-diphenylalanine hydrogel networks', *Materials Science and Engineering C*. Elsevier Ltd, 66, pp. 221–229. doi: 10.1016/j.msec.2016.04.084.

Claudino, W. M. *et al.* (2007) 'Metabolomics: Available results, current research projects in breast cancer, and future applications', *Journal of Clinical Oncology*. American Society of Clinical Oncology, pp. 2840–2846. doi: 10.1200/JCO.2006.09.7550.

CM, H. *et al.* (2013) 'Assessments of Injectable Alginate Particle-Embedded Fibrin Hydrogels for Soft Tissue Reconstruction', *Biomedical materials (Bristol, England)*. Biomed Mater, 8(1). doi: 10.1088/1748-6041/8/1/014105.

Cohen, D. L. *et al.* (2006) 'Direct freeform fabrication of seeded hydrogels in arbitrary geometries', *Tissue Engineering*. Tissue Eng, 12(5), pp. 1325–1335. doi: 10.1089/ten.2006.12.1325.

Daemi, *et al.* (2012) 'Synthesis and characterization of calcium alginate nanoparticles, sodium homopolymannuronate salt and its calcium nanoparticles', *Scientia Iranica*. No longer published by Elsevier, 19(6), pp. 2023–2028. doi: 10.1016/j.scient.2012.10.005.

Dai, X. *et al.* (2016) '3D bioprinted glioma stem cells for brain tumor model and applications of drug susceptibility', *Biofabrication*. IOP Publishing, 8(4). doi: 10.1088/1758-5090/8/4/045005.

Debnath, M. *et al.* (2010a) 'Introduction to Molecular Diagnostics', in *Molecular Diagnostics: Promises and Possibilities*. Springer Netherlands, pp. 1–10. doi: 10.1007/978-90-481-3261-4_1.

Debnath, M. *et al.* (2010b) 'Omics Technology', in *Molecular Diagnostics: Promises and Possibilities*. Springer Netherlands, pp. 11–31. doi: 10.1007/978-90-481-3261-4_2.

DiMasi, *et al*. (2003) 'The price of innovation: new estimates of drug development costs', *Journal of Health Economics*, 22, pp. 151–185. doi: 10.1016/S0167-6296(02)00126-1.

Dimitrov, *et al*. (2006) 'Advances in three dimensional printing - State of the art and future perspectives', *Rapid Prototyping Journal*. Emerald Group Publishing Limited, 12(3), pp. 136–147. doi: 10.1108/13552540610670717.

Double, *et al*. (1989) 'Therapeutic index: a vital component in selection of anticancer agents for clinical trial.', *Journal of the National Cancer Institute*, 81(13), pp. 988–94. doi: 10.1093/jnci/81.13.988.

Elango, J. *et al.* (2019) 'Collagen Peptide Upregulates Osteoblastogenesis from Bone Marrow Mesenchymal Stem Cells through MAPK- Runx2', *Cells*. MDPI AG, 8(5), p. 446. doi: 10.3390/cells8050446.

Fedorovich, N. E. *et al.* (2008) 'Three-dimensional fiber deposition of cell-laden, viable, patterned constructs for bone tissue printing', *Tissue Engineering - Part A.* Mary Ann Liebert Inc., 14(1), pp. 127–133. doi: 10.1089/ten.a.2007.0158.

Fedorovich, N. E. *et al.* (2012) 'Biofabrication of osteochondral tissue equivalents by printing topologically defined, cell-laden hydrogel scaffolds', *Tissue Engineering - Part C: Methods*. Mary Ann Liebert Inc., 18(1), pp. 33–44. doi: 10.1089/ten.tec.2011.0060.

Fidler, I. J., *et al* .(1990) 'Orthotopic implantation is essential for the selection, growth and metastasis of human renal cell cancer in nude mice [corrected].', *Cancer metastasis reviews*, 9(2), pp. 149–65. doi: 10.1007/bf00046341.

Foox, M. *et al.* (2015) 'Drug delivery from gelatin-based systems', *Expert Opinion on Drug Delivery*. Taylor and Francis Ltd, pp. 1547–1563. doi: 10.1517/17425247.2015.1037272.

Frantz, S. *et al*. (2003) 'New drug approvals for 2002', *Nature Reviews Drug Discovery*, pp. 95–96. doi: 10.1038/nrd1014.

Galloway, S. M. (1994) 'Chromosome aberrations induced in vitro: Mechanisms, delayed expression, and intriguing questions', *Environmental and Molecular Mutagenesis*. John Wiley & Sons, Ltd, 23(S2), pp. 44–53. doi: 10.1002/em.2850230612.

Giuseppe, M. Di *et al.* (2018) 'Mechanical behaviour of alginate-gelatin hydrogels for 3D bioprinting', *Journal of the Mechanical Behavior of Biomedical Materials*. Elsevier Ltd, 79, pp. 150–157. doi: 10.1016/j.jmbbm.2017.12.018.

Glavas-Dodov, M. *et al.* (2013) 'Wheat germ agglutinin-functionalised crosslinked polyelectrolyte microparticles for local colon delivery of 5-FU: In vitro efficacy and in vivo gastrointestinal distribution', *Journal of Microencapsulation*. Taylor & Francis, 30(7), pp. 643–656. doi: 10.3109/02652048.2013.770099.

Godoy, P. *et al.* (2012) 'Toxicogenomic-based approaches predicting liver toxicity in vitro', *Archives of Toxicology*. Springer, pp. 1163–1164. doi: 10.1007/s00204-012-0892-5.

GOLDIN, A. *et al.* (1961) 'Evaluation of chemical agents against carcinoma CA-755 in mice.', *Cancer research*, 21, pp. 617–91. Available at: http://www.ncbi.nlm.nih.gov/pubmed/13899777 (Accessed: 22 April 2020).

Gross, B. C. *et al.* (2014) 'Evaluation of 3D Printing and Its Potential Impact on Biotechnology and the Chemical Sciences'. doi: 10.1021/ac403397r.

GS, D. *et al.* (2014) 'Manufacture of β-TCP/alginate Scaffolds Through a Fab@home Model for Application in Bone Tissue Engineering', *Biofabrication*. Biofabrication, 6(2). doi: 10.1088/1758-5082/6/2/025001.

Gu, Q. *et al.* (2015) 'Three-dimensional bio-printing', *Science China Life Sciences*. Science in China Press, 58(5), pp. 411–419. doi: 10.1007/s11427-015-4850-3.

H, M. *et al.* (2015) 'Non-small cell lung cancer 95D cells co-cultured with 3D-bioprinted scaffold to construct a lung cancer model in vitro.', *Zhonghua Zhong liu za zhi [Chinese Journal of Oncology]*, 37(10), pp. 736–740.

Hersel, *et al*. (2003) 'RGD modified polymers: Biomaterials for stimulated cell adhesion and beyond', *Biomaterials*. Elsevier BV, 24(24), pp. 4385–4415. doi: 10.1016/S0142-9612(03)00343-0.

Holbeck, S. L. (2004) 'Update on NCI in vitro drug screen utilities', *European Journal of Cancer*. Elsevier Ltd, 40(6), pp. 785–793. doi: 10.1016/j.ejca.2003.11.022.

Hopp, B. (2012) 'Femtosecond laser printing of living cells using absorbing film-assisted laser-induced forward transfer', *Optical Engineering*. SPIE-Intl Soc Optical Eng, 51(1), p. 014302. doi: 10.1117/1.oe.51.1.014302.

Hsiao, A. Y. *et al.* (2009) 'Microfluidic system for formation of PC-3 prostate cancer co-culture spheroids', *Biomaterials*. Biomaterials, 30(16), pp. 3020–3027. doi: 10.1016/j.biomaterials.2009.02.047.

Hulmes, D. J. S. (2002) 'Building collagen molecules, fibrils, and suprafibrillar structures', in *Journal of Structural Biology*. Academic Press Inc., pp. 2–10. doi: 10.1006/jsbi.2002.4450.

Jain, A. K. *et al.* (2018) 'Models and Methods for In Vitro Toxicity', in *In Vitro Toxicology*. Elsevier Inc., pp. 45–65. doi: 10.1016/B978-0-12-804667-8.00003-1.

Jung, J. W., Lee, J. S. and Cho, D. W. (2016) 'Computer-Aided multiple-head 3D printing system for printing of heterogeneous organ/tissue constructs', *Scientific* Karim, A. A. *et al*. (2009) 'Fish gelatin: properties, challenges, and prospects as an alternative to mammalian gelatins', *Food Hydrocolloids*, pp. 563–576. doi: 10.1016/j.foodhyd.2008.07.002.

Karreth, *et al.* (2009) 'Modelling oncogenic Ras/Raf signalling in the mouse', *Current Opinion in Genetics and Development*, pp. 4–11. doi: 10.1016/j.gde.2008.12.006.

Klebe, R. J. (1988) 'Cytoscribing: A method for micropositioning cells and the construction of two- and three-dimensional synthetic tissues', *Experimental Cell Research*. Exp Cell Res, 179(2), pp. 362–373. doi: 10.1016/0014-4827(88)90275-3.

Kumar, S., *et al.* (2016) 'Preclinical screening methods in cancer', *Indian Journal of Pharmacology*, 48(5), pp. 481–486. doi: 10.4103/0253-7613.190716.

LaBarbera, *et al*.(2012) 'The multicellular tumor spheroid model for high-throughput cancer drug discovery', *Expert Opinion on Drug Discovery*, 7(9), pp. 819–830. doi: 10.1517/17460441.2012.708334.

Lecoeur, H. *et al.* (2001) 'A novel flow cytometric assay for quantitation and multiparametric characterization of cell-mediated cytotoxicity', *Journal of Immunological Methods*, 253(1–2), pp. 177–187. doi: 10.1016/S0022-1759(01)00359-3.

Lee, D. C. *et al.* (2007) '6-Hydroxydopamine induces cystatin C-mediated cysteine protease suppression and cathepsin D activation', *Neurochemistry International*, 50(4), pp. 607–618. doi: 10.1016/j.neuint.2006.12.006.

Leira, F. *et al.* (2002) 'Fluorescent microplate cell assay to measure uptake and metabolism of glucose in normal human lung fibroblasts', *Toxicology in Vitro*, 16(3), pp. 267–273. doi: 10.1016/S0887-2333(02)00002-4.

Lewis, M. (2012) 'Antioxidant Screen for Extracts: DPPH assay', *Natural Product Screening*, 2, pp. 5–7. doi: 10.1007/978-1-4614-9135-4.

Li, C. M. *et al.* (2008) 'Biochips - fundamentals and applications', in *Electrochemical Sensors, Biosensors and their Biomedical Applications*. Elsevier Inc., pp. 307–383. doi: 10.1016/B978-012373738-0.50013-1.

Liu, M. *et al.* (2017) 'Injectable Thermoresponsive Hydrogel Formed by Alginate-g-Poly(N-isopropylacrylamide) That Releases Doxorubicin-Encapsulated Micelles as a Smart Drug Delivery System', *ACS Applied Materials and Interfaces*. American Chemical Society, 9(41), pp. 35673–35682. doi: 10.1021/acsami.7b12849.

Liu, T., Delavaux, C. and Zhang, Y. S. (2019) '3D bioprinting for oncology applications', *Journal of 3D Printing in Medicine*, 3(2), pp. 55–58. doi: 10.2217/3dp-2019-0004.

Lodhia, K. A. *et al.* (2015) 'Prioritizing therapeutic targets using patient-derived xenograft models', *Biochimica et Biophysica Acta - Reviews on Cancer*. Elsevier, pp. 223–234. doi: 10.1016/j.bbcan.2015.03.002.

Ma, P. X. (2004) 'Scaffolds for tissue fabrication', *Materials Today*. Elsevier, 7(5), pp. 30–40. doi: 10.1016/S1369-7021(04)00233-0.

Mahto, S. K., *et al*. (2010) 'In vitro models, endpoints and assessment methods for the measurement of cytotoxicity', *Toxicology and Environmental Health Sciences*, pp. 87–93. doi: 10.1007/BF03216487.

McKeage, *et al.* (2008) 'The potential of DMXAA (ASA404) in combination with docetaxel in advanced prostate cancer', *Expert Opinion on Investigational Drugs*, 17(1), pp. 23–29. doi: 10.1517/13543784.17.1.23.

Di Modugno, F. *et al.* (2019) '3D models in the new era of immune oncology: Focus on T cells, CAF and ECM', *Journal of Experimental and Clinical Cancer Research*. doi: 10.1186/s13046-019-1086-2.

Mondal, A. *et al.* (2019) 'Characterization and printability of Sodium alginate -Gelatin hydrogel for bioprinting NSCLC co-culture', *Scientific Reports*. Nature Research, 9(1), pp. 1–12. doi: 10.1038/s41598-019-55034-9.

Nath, S. *et al*. (2016) 'Three-dimensional culture systems in cancer research: Focus on tumor spheroid model', *Pharmacology and Therapeutics*. Elsevier B.V., 163, pp. 94–108. doi: 10.1016/j.pharmthera.2016.03.013.

Nunes, A. S. *et al.* (2019) '3D tumor spheroids as in vitro models to mimic in vivo human solid tumors resistance to therapeutic drugs', *Biotechnology and Bioengineering*. John Wiley and Sons Inc., pp. 206–226. doi: 10.1002/bit.26845.

Nyga, A., *et al* (2011) '3D tumour models: Novel in vitro approaches to cancer studies', *Journal of Cell Communication and Signaling*. J Cell Commun Signal, pp. 239–248. doi: 10.1007/s12079-011-0132-4.

Oliver, M. H. *et al.* (1989) 'A rapid and convenient assay for counting cells cultured in microwell plates: Application for assessment of growth factors', *Journal of Cell Science*, 92(3), pp. 513–518.

Olson, H. *et al.* (2000) 'Concordance of the toxicity of pharmaceuticals in humans and in animals', *Regulatory Toxicology and Pharmacology*. Academic Press Inc., 32(1), pp. 56–67. doi: 10.1006/rtph.2000.1399.

Orive, G. *et al.* (2002) 'Biocompatibility of microcapsules for cell immobilization elaborated with different type of alginates'. Biomaterials, 23(18), pp. 3825–3831. doi: 10.1016/S0142-9612(02)00118-7.

Parmar, P. A. *et al.* (2015) 'Collagen-mimetic peptide-modifiable hydrogels for articular cartilage regeneration', *Biomaterials*. Elsevier Ltd, 54, pp. 213–225. doi: 10.1016/j.biomaterials.2015.02.079.

Parng, C. *et al.* (2002) 'Zebrafish: a preclinical model for drug screening.', *Assay and drug development technologies*, 1(1 Pt 1), pp. 41–48. doi:

10.1089/154065802761001293.

Pawlik, A. *et al.* (2016) 'Cytoskeletal reorganization and cell death in mitoxantrone-treated lung cancer cells', *Acta Histochemica*. Elsevier GmbH., 118(8), pp. 784–796. doi: 10.1016/j.acthis.2016.10.001.

R, C. *et al.* (2010) 'Biofabrication of a Three-Dimensional Liver Micro-Organ as an in Vitro Drug Metabolism Model', *Biofabrication*. Biofabrication, 2(4). doi: 10.1088/1758-5082/2/4/045004.

Ramezani Kalmer, R. *et al.* (2019) 'Fabrication and evaluation of carboxymethylated diethylaminoethyl cellulose microcarriers as support for cellular applications', *Carbohydrate Polymers*. Elsevier, 226(September), p. 115284. doi: 10.1016/j.carbpol.2019.115284.

Reddivari, L. *et al.* (2007) 'Anthocyanin fraction from potato extracts is cytotoxic to prostate cancer cells through activation of caspase-dependent and caspase-independent pathways.', *Carcinogenesis*, 28(10), pp. 2227–35. doi: 10.1093/carcin/bgm117.

Roudsari, *et al*. (2018) 'Lung Adenocarcinoma Cell Responses in a 3D in Vitro Tumor Angiogenesis Model Correlate with Metastatic Capacity', *ACS Biomaterials Science and Engineering*, 4(2), pp. 368–377. doi: 10.1021/acsbiomaterials.7b00011.

Rui Yao *et al.* (2009) 'In Vitro Angiogenesis of 3D Tissue Engineered Adipose Tissue', *Journal of Bioactive and Compatible Polymers*. SAGE PublicationsSage UK: London, England, 24(1), pp. 5–24. doi: 10.1177/0883911508099367.

Sanden, K. W. *et al.* (2019) 'The use of Fourier-transform infrared spectroscopy to characterize connective tissue components in skeletal muscle of Atlantic cod (*Gadus morhua* L.)', *Journal of Biophotonics*. Wiley-VCH Verlag, 12(9). doi: 10.1002/jbio.201800436.

Sarker, B. *et al.* (2014) 'Fabrication of alginate-gelatin crosslinked hydrogel microcapsules and evaluation of the microstructure and physico-chemical properties', *Journal of Materials Chemistry B*. The Royal Society of Chemistry, 2(11), pp. 1470–1482. doi: 10.1039/c3tb21509a.

Sarker, B. *et al.* (2017) 'Macromolecular interactions in alginate-gelatin hydrogels regulate the behavior of human fibroblasts', *Journal of Bioactive and Compatible Polymers*. SAGE Publications Ltd, 32(3), pp. 309–324. doi: 10.1177/0883911516668667.

Van Schaik, R. H. N. (2005) 'Cancer treatment and pharmacogenetics ofcytochrome P450 enzymes', *Investigational New Drugs*, pp. 513–522. doi: 10.1007/s10637-005-4019-1.

Shengjie Li *et al.* (2009) 'Direct Fabrication of a Hybrid Cell/Hydrogel Construct by a Double-nozzle Assembling Technology', *Journal of Bioactive and Compatible Polymers*. SAGE PublicationsSage UK: London, England, 24(3), pp. 249–265. doi: 10.1177/0883911509104094.

Simian, M. *et al.* (2017) 'Organoids: A historical perspective of thinking in three dimensions', *Journal of Cell Biology*. Rockefeller University Press, 216(1), pp. 31–40. doi: 10.1083/jcb.201610056.

Skehan, P. *et al.* (1990) 'New colorimetric cytotoxicity assay for anticancer-drug screening', *Journal of the National Cancer Institute*, 82(13), pp. 1107–1112. doi: 10.1093/jnci/82.13.1107.

Smith, J. A. (1982) 'Scanning electron microscopy', *Physics Education*, 17(3), pp. 111–114. doi: 10.1088/0031-9120/17/3/304.

Soldatow, V. Y. *et al.* (2013) 'In vitro models for liver toxicity testing', *Toxicology Research*, 2(1), pp. 23–39. doi: 10.1039/c2tx20051a.

Sutherland, R. M. (1988) 'Cell and environment interactions in tumor microregions: The multicell spheroid model', *Science*. Science, pp. 177–184. doi: 10.1126/science.2451290.

Szadvari, I., *et al.* (2016) 'Athymic nude mice as an experimental model for cancer treatment', *Physiological Research*, 65, pp. S441–S453. doi: 10.33549/physiolres.933526.

Talbot, E. L. *et al.* (2012) 'Evaporation of picoliter droplets on surfaces with a range of wettabilities and thermal conductivities', *Physical Review E - Statistical, Nonlinear, and Soft Matter Physics*. Phys Rev E Stat Nonlin Soft Matter Phys, 85(6). doi: 10.1103/PhysRevE.85.061604.

Tønnesen, *et al.* (2002) 'Alginate in drug delivery systems', *Drug Development and Industrial Pharmacy*. Drug Dev Ind Pharm, pp. 621–630. doi: 10.1081/DDC-120003853.

Vaira, V. *et al.* (2010) 'Preclinical model of organotypic culture for pharmacodynamic profiling of human tumors', *Proceedings of the National Academy of Sciences of the United States of America*. Proc Natl Acad Sci U S A, 107(18), pp. 8352–8356. doi: 10.1073/pnas.0907676107.

Valot, L. *et al.* (2019) 'Chemical insights into bioinks for 3D printing', *Chemical Society Reviews*. Royal Society of Chemistry, 48(15), pp. 4049–4086. doi: 10.1039/c7cs00718c.

Vanderhooft, *et al.* (2007) 'Synthesis and characterization of novel thiol-reactive poly(ethylene glycol) cross-linkers for extracellular-matrix-mimetic biomaterials', *Biomacromolecules*. Biomacromolecules, 8(9), pp. 2883–2889. doi: 10.1021/bm0703564.

Velasquillo, C. *et al.* (2013) 'Skin 3D Bioprinting. Applications in Cosmetology', *Journal of Cosmetics, Dermatological Sciences and Applications*, (3), pp. 85–89. doi: 10.4236/jcdsa.2013.31A012.

Venditti, J. M., *et al.* (1984) 'Current NCl preclinical antitumor screening in vivo: Results of tumor panel screening, 1976-1982, and future directions', *Advances in Pharmacology and Chemotherapy*, VOL. 20, pp. 1–20. doi: 10.1016/s1054-3589(08)60263-x.

Venkatesh, N. *et al.* (2004) 'Chemical genetics to identify NFAT inhibitors: Potential of targeting calcium mobilization in immunosuppression', *Proceedings of the National Academy of Sciences of the United States of America*, 101(24), pp. 8969–8974. doi: 10.1073/pnas.0402803101.

Wang, X. *et al.* (2017) 'Gelatin-based hydrogels for organ 3D bioprinting', *Polymers*. MDPI AG, p. 401. doi: 10.3390/polym9090401.

Wang, X. *et al.* (2018) 'Tumor-like lung cancer model based on 3D bioprinting', *3 Biotech*. Springer International Publishing, 8(12), pp. 1–9. doi: 10.1007/s13205-018-1519-1.

Wang, Y. *et al.* (2018) '3D Bioprinting of Breast Cancer Models for Drug Resistance Study', *ACS Biomaterials Science and Engineering*. American Chemical Society, 4(12), pp. 4401–4411. doi: 10.1021/acsbiomaterials.8b01277.

Weiss, *et al.* (2003) 'Mouse cancer models as a platform for performing preclinical therapeutic trials.', *Current opinion in genetics & development*, 13(1), pp. 84–9. doi: 10.1016/s0959-437x(02)00016-3.

Wen, X. *et al.* (2015) 'Immobilization of collagen peptide on dialdehyde bacterial cellulose nanofibers via covalent bonds for tissue engineering and regeneration', *International Journal of Nanomedicine*. Dove Medical Press Ltd., 10, pp. 4623–4637. doi: 10.2147/IJN.S84452.

Xiao, C. *et al.* (2001) 'BLEND FILMS FROM SODIUM ALGINATE AND GELATIN SOLUTIONS', *Journal of Macromolecular Science, Part A*. Taylor & Francis Group , 38(3), pp. 317–328. doi: 10.1081/MA-100103352.

Xu, T. *et al.* (2005) 'Inkjet printing of viable mammalian cells', *Biomaterials*. Biomaterials, 26(1), pp. 93–99. doi: 10.1016/j.biomaterials.2004.04.011.

Xu, T. *et al.* (2013) 'Complex heterogeneous tissue constructs containing multiple cell types prepared by inkjet printing technology', *Biomaterials*. Biomaterials, 34(1), pp. 130–139. doi: 10.1016/j.biomaterials.2012.09.035.

Yakisich, J. S. (2012) 'An Algorithm for the Preclinical Screening of Anticancer Drugs Effective against Brain Tumors', *ISRN Pharmacology*, 2012, pp. 1–5. doi: 10.5402/2012/513580.

Yan, Y. *et al.* (2005) 'Fabrication of viable tissue-engineered constructs with 3D cell-assembly technique', *Biomaterials*. Biomaterials, 26(29), pp. 5864–5871. doi:

10.1016/j.biomaterials.2005.02.027.

Zhang, X. L. *et al.* (2006) 'Construction of in vitro multicellular tumor spheroid model with microencapsulation and its application in anticancer drug screening', *Chinese Journal of Clinical Rehabilitation*, 10(17), pp. 72–75.

Zhao, Y. *et al.* (2014) 'Three-dimensional printing of Hela cells for cervical tumor model in vitro', *Biofabrication*, 6(3). doi: 10.1088/1758-5082/6/3/035001.

Zucco, F. *et al.* (2004) 'Toxicology investigations with cell culture systems: 20 Years after', *Toxicology in Vitro*. Elsevier Ltd, 18(2), pp. 153–163. doi: 10.1016/S0887-2333(03)00147-4.